Ecohydrology

Transpiration from subarctic deciduous woodlands: environmental controls and contribution to ecosystem evapotranspiration

Journal:	*Ecohydrology*
Manuscript ID	ECO-19-0070.R1
Wiley - Manuscript type:	Research Article
Date Submitted by the Author:	10-Nov-2019
Complete List of Authors:	Sabater, Ana Maria; Universitat Autònoma de Barcelona; CREAF; University of Alicante; CEAM Ward, Helen; University of Innsbruck, Department of Atmospheric and Cryospheric Sciences Hill, Tim; University of Exeter, Department of Geography Gornall, Jemma; Met Office Wade, Thomas; The University of Edinburgh Evans, Jonathan; Centre for Ecology and Hydrology Prieto-Blanco, Ana; UCL Disney, Mathias; UCL; NCEO Phoenix, Gareth; The University of Sheffield Williams, Mathew; The University of Edinburgh Huntley, Brian; Durham University Baxter, Robert; Durham University Mencuccini, Maurizio; ICREA; CREAF Poyatos, Rafael; CREAF; Universitat Autonoma de Barcelona; Ghent University
Keywords:	Arctic, branch cuvettes, eddy covariance, evapotranspiration partitioning, mountain birch, tundra, understorey, boreal forest

Transpiration from subarctic deciduous woodlands: environmental controls and contribution to ecosystem evapotranspiration.

Ana M. Sabater [1,2,3,4], Helen C. Ward [5], Timothy C. Hill [6], Jemma L. Gornall[7], Thomas J. Wade [8], Jonathan G. Evans [9], Ana Prieto-Blanco [10], Mathias Disney [10, 11], Gareth K. Phoenix [12], Mathew Williams [8], Brian Huntley [13], Robert Baxter [13], Maurizio Mencuccini [2, 14], Rafael Poyatos [1, 2, 15]

[1] Universitat Autònoma de Barcelona, Barcelona, Spain.

[2] CREAF, Cerdanyola del Vallès, Barcelona, Spain.

[3] Fundación CEAM, Joint Research Unit University of Alicante-CEAM, Alicante, Spain.

[4] Department of Ecology, University of Alicante, Alicante, Spain.

[5] Department of Atmospheric and Cryospheric Sciences (ACINN), University of Innsbruck, Innsbruck, Austria.

[6] College of Life and Environmental Sciences, Department of Geography, University of Exeter, Exeter, UK.

[7] Met Office, Exeter, UK.

[8] School of Geosciences, University of Edinburgh, Edinburgh, UK.

[9] Centre for Ecology and Hydrology, Wallingford, UK.

[10] University College London, Department of Geography, London, UK.

[11] NERC National Centre for Earth Observation (NCEO), Leicester, UK.

[12] Department of Animal and Plant Sciences, University of Sheffield, Sheffield, UK.

[13] Department of Biosciences, Durham University, Durham, UK.

[14] ICREA, Barcelona, Spain.

[15] Laboratory of Plant Ecology, Faculty of Bioscience Engineering, Ghent University, Ghent, Belgium.

Correspondence. R. Poyatos, CREAF, Edifici C, Campus UAB Bellaterra, E08193 Barcelona, Spain. Email: r.poyatos@creaf.uab.es, Tel.+34 935814676, Fax: +34935814151.

Short title: Transpiration and evapotranspiration of subarctic deciduous woodlands

Abstract

Potential land-climate feedbacks in subarctic regions, where rapid warming is driving forest expansion into the tundra, may be mediated by differences in transpiration of different plant functional types. Here we assess the environmental controls of overstorey transpiration and its relevance for ecosystem evapotranspiration in subarctic deciduous woodlands. We measured overstorey transpiration of mountain birch canopies and ecosystem evapotranspiration in two locations in northern Fennoscandia, having dense (Abisko) and sparse (Kevo) overstories. For Kevo, we also upscale chamber-measured understorey evapotranspiration from shrubs and lichen using a detailed land cover map. Sub-daily evaporative fluxes were not affected by soil moisture, and showed similar controls by vapour pressure deficit and radiation across sites. At the daily timescale, increases in evaporative demand led to proportionally higher contributions of overstorey transpiration to ecosystem evapotranspiration. For the entire growing season, the overstorey transpired 33% of ecosystem evapotranspiration in Abisko and only 16% in Kevo. At this latter site, the understorey had a higher leaf area index and contributed more to ecosystem evapotranspiration compared to the overstorey birch canopy. In Abisko, growing season evapotranspiration was 27% higher than precipitation, consistent with a gradual soil moisture depletion over the summer. Our results show that overstorey canopy transpiration in subarctic deciduous woodlands is not the dominant evaporative flux. However, given the observed environmental sensitivity of evapotranspiration components, the role of deciduous trees in driving ecosystem evapotranspiration may increase with the predicted increases in tree cover and evaporative demand across subarctic regions.

Keywords

Arctic, branch cuvettes, eddy covariance, evapotranspiration partitioning, mountain birch, tundra, understorey

Introduction

Northern high latitudes (boreal and arctic biomes) exert an important influence in global biosphere-atmosphere interactions involving water, energy and atmospheric composition. These interactions are globally relevant because of the large extent of these biomes (arctic tundra and boreal forest cover *ca.* $1.24 \cdot 10^8$ km^2) and the intense and rapid warming occurring at northern high latitudes (0.5 K/decade since 1979; IPCC, 2013), which is partly driven by regional positive feedbacks (Chapin et al., 2000). Warmer temperatures and longer growing seasons are already inducing poleward and altitudinal treeline migration and shrub expansion in the tundra zone, which may in turn drive considerable land-atmosphere feedbacks in these latitudes (Kattsov et al., 2005; Swann, Fung, Levis, Bonan, & Doney, 2010; Zhang et al., 2013)

Treelines across the subarctic vegetation belt are largely dominated by conifers, although deciduous broadleaves occupy 18% of the forest area at latitudes above 60º across Eurasia (Krankina et al., 2010) and can form the tundra-to-forest transition in many subarctic regions with oceanic influence (Callaghan et al., 2005). The area of deciduous broadleaf woodlands is increasing throughout the subarctic region (Hofgaard, Tømmervik, Rees, & Hanssen, 2013; Rundqvist et al., 2011; Tømmervik et al., 2004; Wang et al., 2019), following a general trend of increasing deciduous vegetation at northern high latitudes (Myers-Smith et al., 2011). These vegetation changes are predicted to continue in the future (Mekonnen, Riley, Randerson, Grant, & Rogers, 2019) and may cause substantial land-climate feedbacks mediated by changes in albedo, in carbon sequestration and in evaporative fluxes (Bonan, 2008; Bonfils et al., 2012). Higher transpiration rates by deciduous broadleaf forests could lead to stronger evaporative cooling locally (Chapin et al., 2000), although, in a regional context, the effects of the expansion of deciduous broadleaf trees into the tundra zone can be more complex and actually enhance Arctic warming (Swann et al., 2010). Moreover, increased soil moisture uptake by deciduous trees could lead to faster depletion of snowmelt water during the shoulder season, triggering further hydrological changes (Young-Robertson, Bolton, Bhatt, Cristóbal, & Thoman, 2016). Therefore, a greater understanding of the magnitudes and controls of evapotranspiration in deciduous woodlands is needed to predict future changes in land-atmosphere interactions in subarctic forest-tundra ecotones.

Syntheses addressing magnitudes and drivers of ecosystem evapotranspiration (ET_{eco}) at northern high latitudes show a paucity of data for deciduous broadleaf forests from subarctic locations (Brümmer et al., 2011; Kasurinen et al., 2014; McFadden, Eugster, & Chapin III, 2003). These syntheses show that leaf area index (LAI), meteorological conditions and physiological regulation by vegetation are the three major factors affecting ET_{eco} in northern high-latitude ecosystems. In these ecosystems, evapotranspiration is largely driven by vapour pressure deficit (VPD), radiation and temperature, with soil moisture often playing a minor role (Beringer, Chapin, Thompson, & McGuire, 2005; Brümmer et al., 2011). In deciduous forests, growing season duration also affects seasonal evapotranspiration through the influence on LAI phenology (Brümmer et al., 2012). Deciduous broadleaf forests from northern high latitudes show higher evapotranspiration rates compared to conifer forests in the same region (Brümmer et al., 2011; Kasurinen et al., 2014), but they may also display a stronger stomatal control with increasing VPD (Welp, Randerson, & Liu, 2007). However, to what extent do these patterns in the drivers of ET_{eco} from northern high-latitude deciduous forests reflect the transpiration regulation by the main canopy?

The partitioning of ET_{eco} into transpiration and evaporation and the factors controlling this partitioning are still poorly known (Schlesinger & Jasechko, 2014). Subarctic and northern boreal woodlands typically show a low LAI of the dominant canopy species, meaning that the contribution of understorey and soil evaporation to ecosystem evapotranspiration may be moderate to high (Blanken et al., 2001; Iida et al., 2009; Lafleur, 1992), although it will depend on vegetation structure (Beringer et al., 2005). This substantial contribution of the soil and understorey to ET_{eco} implies that eddy flux-based estimates of ET_{eco} in these forests may well represent the mix of physical and biological controls on evaporative fluxes and will only partially capture the physiological regulation exerted by the main canopy (Ikawa et al., 2015; Kasurinen et al., 2014). Evaporative fluxes of overstorey, understorey and the forest floor may have contrasting hydroclimatic responses (Iida et al., 2009) and a strong seasonal variation (Blanken et al., 2001). Although several studies have addressed the magnitudes and drivers of the different components of ET_{eco} in northern boreal and subarctic forests (Blanken et al., 2001; Grelle, Lundberg, Lindroth, Morén, & Cienciala, 1997; Iida et al., 2009; Ikawa et al., 2015), we are not aware of any study of these characteristics from subarctic deciduous woodlands.

In this article, we quantify the magnitude and seasonal controls on ET_{eco} and on the transpiration of the main canopy in two deciduous broadleaf woodlands dominated by mountain birch (*Betula pubescens* spp. *czerepanovii* (Orlova) Hamet- Ahti). This is a representative species of subarctic woodlands covering 600000 ha throughout northern Fennoscandia (Haapanala et al., 2009). The Abisko site (N Sweden) displays a denser birch woodland compared to the sparser Kevo site (N Finland), which is also slightly colder and wetter. Therefore, the Abisko woodland would be representative of denser canopies which are becoming common across the subarctic in response to warming and reduced browsing (Callaghan et al., 2013). In both sites, we measured ET_{eco} and birch transpiration per leaf area (T_{leaf}), which was upscaled to the birch canopy level (T_{birch}). Our main goals were: (1) to identify the drivers of ET_{eco} and T_{leaf}, to understand the environmental controls between the two scales (ecosystem vs branch) and at sites, which differed substantially in stand structure (denser in Abisko, sparser in Kevo); and (2) to investigate how variation in canopy structure affects growing season values of ET_{eco} relative to growing season precipitation and to quantify the contribution of T_{birch} to ET_{eco}. To further understand this evapotranspiration partitioning in subarctic deciduous woodlands, at Kevo we also upscaled evaporative fluxes from birch and understorey ($ET_{upscaled}$) to explore how this variable compares to ET_{eco}.

2. Methodology

2.1. Study sites

Two mountain birch (*Betula pubescens* ssp. *czerepanovii*) forest sites within the northern Fennoscandia sub-Artic vegetation belt were chosen for this study: Abisko (northern Sweden) and Kevo (northern Finland). Both sites were located near the mountain birch/tundra ecotone, where mountain birches are polycormic because of the harsh environmental conditions and the frequent defoliation by autumn and winter moths (*Epirrita autumnata* and *Operophtera brumata*). At both sites, we measured transpiration of mountain birch branches, ecosystem evapotranspiration and other environmental drivers during the mountain birch leaf-on period, hereby abbreviated as 'growing season', of 2007 (Abisko, DOY 153-241) and of 2008 (Kevo, DOY 171-257).

In Abisko (Figure 1a), measurements were undertaken at a location (68.326°N, 18.833°E, 519 m.a.s.l) *ca.* 3.2 km south-east of the Abisko Research Station. At the study site, mean annual temperature is -0.9ºC and mean annual precipitation is 335 mm (1980-2010, temperature corrected assuming a lapse rate of 0.55 ºC per 100 m of elevation). The predominant substrate is coarse glacial till and soils are typically micro-podzols, with no permafrost present (Hartley, Hopkins, Sommerkorn, & Wookey, 2010). The landscape presents a relatively complex topography, which results in highly variable forest cover (Nyström, Holmgren, & Olsson, 2012) and stand structures (Table 1). Understorey vegetation is dominated by the dwarf shrubs *Empetrum nigrum* ssp *hermaphroditum, Vaccinium myrtillus* and *Vaccinium uliginosum* (Hartley et al., 2010; Poyatos, Gornall, Mencuccini, Huntley, & Baxter, 2012).

In Kevo (Figure 1b), measurements were undertaken at a location (69.492°N, 27.234°E, 260 m.a.s.l.) *ca*. 40 km south of the Kevo Subartic Research Institute. Climate at the site (1978-2007, data from the the Kevo Institute station, corrected for lapse rate) is colder and wetter than in Abisko (-2.4ºC and 422 mm mean annual temperature and precipitation, respectively) and the substrate is composed of gneiss covered by glacial till, and no permafrost is present at the forest site. Mountain birch forests in Kevo, located upon gentle slopes/ridges and surrounded by mires in topographically depressed areas, were sparser and showed a more homogeneous structure compared to Abisko (Table 1). Understorey vegetation showed a higher LAI compared to Abisko (Table 1); it consisted of *E. nigrum* below mountain birch canopies and distinct patches covered by *Betula nana* L. and *Cladonia* spp, lichens in the open areas (Poyatos et al., 2012).

One forest inventory was established in the vicinity of each of the branch bags sites to quantify stand structure at the plot level (a 10-m circular plot in Abisko and a 30 x 30 m plot in Kevo). Another set of 30 x 30 m plots was measured in Abisko (N = 5) and Kevo (N = 7) to quantify ecosystem-level stand structure and maximum leaf area index, $\mathrm{LAI}_{\mathrm{max}}$ (m^2 leaf m^{-2}ground). Forest inventory plots were at an average distance from the eddy flux tower of 105 m in Abisko and 450 m in Kevo. Diameters and heights of all stems with diameter at breast height DBH>12 mm within the plots were measured in 2007 at Abisko and in 2008 at Kevo. For Abisko, we used published allometric equations predicting leaf biomass from stem basal area and height (Dahlberg, Berge, Petersson, & Vencatasawmy, 2004) to convert leaf biomass supported by each stem into leaf area using site-specific leaf mass per area. For Kevo, we harvested N = 15 stems during the peak growing season in 2008, to measure their leaf area and we obtained site-specific allometries between stem diameter and leaf area (Table S1). Understorey LAI_{max} was obtained from 1 m^2 vegetation surveys (N = 5) in each of the sites, following Fletcher et al. (2012).

2.2. Branch-level transpiration measurements

At both sites, we selected eight mountain birch branches representative of low and mid-canopy conditions for branch transpiration measurements. Branch transpiration was measured using a multiplexed branch bag device based on the closed system approach (Rayment & Jarvis, 1999; Wingate, Seibt, Moncrieff, Jarvis, & Lloyd, 2007). This system measures water vapour concentration changes within eight 0.11 m^3 ventilated cuvettes enclosing individual branches during 7.5 minutes. Branches were measured sequentially, and a measurement cycle of all eight branches was completed within an hour. During each measurement period, air temperature, T (ºC), relative humidity, RH (%), and photosynthetically active radiation, PAR (μmols photons m^{-2} s^{-1}), were recorded every 5 seconds by a datalogger. The system also recorded the value of environmental variables at the beginning of each transpiration observation (i.e. hourly). The subscript 'branch' was used to refer to branch-level meteorological variables (PAR_{branch}, VPD_{branch}). Further technical details of the branch bags system and of the calculation of branch-level transpiration can be found in the Supporting Information S2.

We quantified branch transpiration on a leaf area basis, T_{leaf} (l m^{-2} $hour^{-1}$), by dividing whole-branch transpiration by the leaf area of the branch within the bag. To account for seasonal variation in branch leaf area, we periodically counted the number of leaves inside the bags during the growing season. We then multiplied the leaf counts by an estimation of the average leaf area obtained from a sample of leaves (N = 10) close to the measured branch, fitted a nonlinear response as a function of day of year and, if needed, corrected by differences in leaf size between inside and outside the bags

(Poyatos et al., 2012). We expressed the seasonal variation in leaf area in relative terms between 0 and 1 (minimum and maximum leaf area, respectively) to use for the upscaling of branch transpiration fluxes.

2.3. Ecosystem evapotranspiration and environmental monitoring

At both sites, half-hourly ecosystem evapotranspiration, ET_{eco} (mm h^{-1}), was estimated from latent heat measurements using the eddy covariance (EC) technique in flux towers located above the mountain birch canopy (Aubinet, Vesala, & Papale, 2012). The three components of wind speed were measured with a sonic anemometer (R3, Gill Instruments, Lymington, UK) and water vapour concentrations were measured by an open-path infrared gas analyser (LI-7500, LI-COR Biosciences, Lincoln, USA). Raw data were logged at 20 Hz and processed to 30-minute statistics using FluxView (Centre for Ecology and Hydrology, Wallingford, UK) and quality-controlled following standard procedures. These include correcting sonic data for angle-of-attack (Gash & Dolman, 2003), compensating for the lag time between sonic and gas analyser, rotating the co-ordinate system (so that the horizontal wind vector is aligned with the 30-min mean and the vertical component is forced to zero), correcting sonic temperature for humidity (Schotanus, Nieuwstadt, & De Bruin, 1983), correcting the fluxes for high- and low- frequency spectral losses and correcting gas fluxes for density effects (Webb, Pearman, & Leuning, 1980). Quality control involved despiking and removal of data outside physically reasonable limits, when instruments malfunctioned, when the windows of the gas analyser were wet or dirty, and during periods of heavy rain. Filtering of data during low turbulence conditions based on a friction velocity threshold was not applied. Energy balance closure was within the expected range (Stoy et al., 2013) and did not differ much across sites (Supplementary Information S3).

Meteorological stations installed at the flux towers measured half-hourly values of temperature, relative humidity, PAR and precipitation above the birch canopy and we refer to them using the subscript ‘eco’ (PAR_{eco}, VPD_{eco}). Soil volumetric water content in the upper 30 cm of the soil, SWC (cm^3 cm^{-3}), was measured with 1 or 2 frequency domain reflectometers (CS616, Campbell Scientific, UK) at each site. To account for site-specific differences in maximum and minimum water-holding capacity, we transformed SWC into soil moisture deficit (SMD), which ranged from 0 (maximum soil moisture) to 1 (minimum soil moisture) (Granier & Loustau, 1994).

2.4. Modelling environmental controls of evaporative fluxes

Firstly, T_{leaf} and ET_{eco} data were filtered (PAR > 50 μmol photons m^{-2} s^{-1}) to avoid noisy vapour concentration data in the branch bags and low turbulence conditions in the case of EC. For T_{leaf}, the values of the meteorological drivers were measured locally in each individual branch (VPD$_{branch}$, PAR$_{branch}$) and for ET_{eco} they were measured above the canopy (VPD$_{eco}$, PAR$_{eco}$).

All models were fitted using the nlme package (Pinheiro, Bates, DebRoy, Sarkar, & R Core Team, 2018) in R (R Core Team 2016). T_{leaf} was modelled using a linear mixed effects model (lme), with VPD$_{branch}$, PAR$_{branch}$ and SMD as fixed factors and ET_{eco} was fitted as a function of VPD$_{eco}$, PAR$_{eco}$ and SMD using a generalized least squares model (gls). In view of the residual distributions after preliminary analyses, we log-transformed the response variables, T_{leaf} and ET_{eco}, and the explanatory variables, except for the case of PAR in ET_{eco} modelling. All models included a first-order autoregressive correlation structure for the residuals, specifying fractional day of year as a continuous time covariate. We applied model selection to include those terms which minimised the value of the Akaike Information Criterion (AIC) while checking that variance inflation factors were below 10 (Zuur, Ieno, & Elphick, 2010). Model selection was carried out with models fitted using maximum likelihood, but final models were fitted using restricted maximum likelihood (Pinheiro & Bates, 2000). Normality, linearity and homoscedasticity of residuals were visually inspected and temporal autocorrelation was analysed visually by autocorrelation plots using the *acf* function in R. We calculated marginal and conditional R^2, the proportion of variance explained by fixed and by both fixed and random factors, respectively (Nakagawa & Schielzeth, 2013).

2.5. Overstorey contributions to ecosystem evapotranspiration

Before upscaling, evaporative flux data were aggregated at the daily scale, using models obtained in section 2.4 to gap-fill missing hourly data and fitting daily models when meteorological data from the measurement systems were missing (Supporting Information S4). We obtained transpiration of the mountain birch canopy, T_{birch} (mm day^{-1}), by multiplying T_{leaf} by the LAI of mountain birch in each stand (Table 1), corrected for seasonal variation (see section 2.2). The calculation was done using mean and ± standard error (SE) of the LAI values, to propagate the uncertainty of the LAI values at each site into the upscaled estimates of T_{birch}.

At both sites we calculated the mountain birch contribution to daily ecosystem evapotranspiration, T_{birch}/ET_{eco} (%). We analysed T_{birch}/ ET_{eco} as a separate linear model of VPD, PAR (both log-transformed) and SMD, including a factor coding for site (Abisko and Kevo) which interacted with each of the environmental drivers. Model selection was carried out based on AIC, as described in section 2.4. We also tested for a possible influence of interception and subsequent canopy evaporation on T_{birch}/ ET_{eco} by testing for differences between dry and wet days, using a gls model as described in the previous paragraph. We considered wet days as those within 2 days after a precipitation event > 1 mm, assuming all wet surfaces would have dried up during this period (Knauer, Werner, & Zaehle, 2015).

Growing season values (mm) of precipitation (*P*), T_{birch}, ET_{eco} and $ET_{upscaled}$ were calculated by aggregating daily values. We also quantified the overall growing season contribution of T_{birch} and $ET_{upscaled}$ to ET_{eco} and expressed growing season evaporative fluxes as a percentage of growing season precipitation.

2.6. Upscaling evapotranspiration components in Kevo

In Kevo, measurements of evapotranspiration were available for other ecosystem components, i.e., understorey shrubs and lichen (Table S3, Figure 1). These evapotranspiration measurements were representative of small patches and were obtained with an automated chamber system (Poyatos et al., 2014) operated during the 2008 growing season, in a forest-mire ecotone *ca.* 200 m from the flux tower (Figure 1). Hourly evapotranspiration of 12 tundra plots was calculated similarly to branch bags fluxes (Supporting Information S5). Because of microclimatic alterations, water vapour sorption in the tubing system and imperfect chamber sealing the automated chamber system used here has been reported to underestimates the evaporative fluxes (Cohen et al., 2015). Therefore, we applied a correction factor of 2.3, obtained in that study, which used a similar device under comparable environmental conditions (Cohen et al., 2015).

Shrub evapotranspiration (ET_{shrub}) was estimated as the mean of N = 9 plots (mean LAI_{max} ± SE = 0.77 ± 0.2) with dwarf tundra vegetation (mainly *Empetrum* *hermaphroditum*, *Calluna vulgaris* and *Vaccinium* spp.) while lichen evaporation (ET_{lichen}) was calculated as the mean of N = 3 lichen heath plots (Poyatos et al., 2014). We then combined evapotranspiration of the individual components with the fractional covers (f) of each component within the footprint of the flux tower. Fractional covers were obtained from aerial photography obtained in August 2008 and subsequent vegetation classification (Hartley et al., 2015). We used a dynamic footprint approach (Hartley et al., 2015) to obtain f values which varied with atmospheric conditions, although results were comparable to those using a simpler, fixed footprint approach (Figure S4). We calculated $ET_{upscaled}$ (mm day^{-1}) as the product of the time-variable f of each component and its corresponding T or ET value:

$$ET_{upscaled} = T_{birch} + f_{birch} \cdot ET_{shrub} + f_{shrub} \cdot ET_{shrub} + f_{lichen} \cdot ET_{lichen} \qquad (1)$$

Where f_{birch}, f_{shrub} and f_{lichen} represent the fractional covers of birch forest, understorey shrubs and lichen, respectively. This equation assumes that shrubs were also typically present under the birch canopies (cf. section 2.1) and that components other than birch, shrubs and lichen (around 5% of fractional cover, Table S3) behave similarly to shrubs.

3. Results

3.1. Temporal variation of environmental variables and evaporative fluxes

Evaporative demand (Figure 2a-d) was higher in Abisko than in Kevo, as shown by higher mean growing season values (± standard deviation, SD) of air temperatures (10.5 °C ± 3.8 and 9.5 °C ± 3.6, respectively), VPD_{eco} (0.5 ± 0.3 kPa and 0.3 ± 0.2 kPa) and PAR_{eco} (407.0 ± 170.0 µmol m^{-2} s^{1} and 260.4 ± 130.3 µmol m^{-2} s^{1}). Light transmission through the birch canopy was higher in Kevo: PAR_{branch}/PAR_{eco} was 56% in Kevo compared to 30% in Abisko (Figure 2a,b). This was associated with the larger difference between VPD_{branch} and VPD_{eco} (Figure 2c,d) in Kevo (average VPD_{branch} - VPD_{eco} = 0.30 kPa) compared to Abisko (average VPD_{branch} - VPD_{eco} = 0.14 kPa). Kevo also received heavier and more frequent precipitation (Figure 2e,f), resulting in higher total growing season precipitation (167.5 mm) compared to Abisko (126.6 mm).

Both T_{leaf} and ET_{eco} tended to be higher in Abisko than in Kevo, on average 50% higher for T_{leaf} and 62% higher for ET_{eco}. Their seasonal dynamics were similar and followed the course of evaporative demand (Figure 2g-j). However, some differences between T_{leaf} and ET_{eco} during the early growing season (before DOY 160) were apparent for Abisko. The diurnal cycles of evaporative fluxes and their drivers varied seasonally in both sites (Figure S2, S3), as expected due to the changing daylight hours at these latitudes. Abisko typically presented higher ET_{eco} and T_{leaf} except during the late season, when T_{leaf} was equal for the two sites.

3. 2. Modelling environmental controls of evaporative fluxes

ET_{eco} and T_{leaf} increased with PAR and VPD but the relationship with VPD showed much less scatter (Figure 3). In general, T_{leaf} and ET_{eco} at a given value of PAR or VPD were higher for Abisko. Models of ET_{eco} and T_{leaf} showed a good predictive ability, with marginal R^2 values > 0.7 (Table 2,3). Model predictors included a negative interaction between PAR and VPD but did not include SMD (Table 2,3). The environmental responses of ET_{eco} did not vary across sites and we only detected site differences for the intercept and the PAR coefficient in the T_{leaf} model (Table 2,3). In both models, the interaction between VPD and PAR resulted in complex patterns in the variation of T_{leaf} and ET_{eco} (Figure 4). For example, for T_{leaf}, steeper relationships with $\mathrm{VPD_{branch}}$ were predicted at low $\mathrm{PAR_{branch}}$ in both sites. In Abisko, higher ET_{eco} was predicted under conditions of high $\mathrm{PAR_{eco}}$ and low $\mathrm{VPD_{eco}}$ values (Figure 4).

3. 3. Overstorey and understorey contributions to ecosystem evapotranspiration

Higher spatial variability of LAI in Abisko (Table 1) translated into a much larger variability in T_{birch}, while T_{birch} was lower and less variable in Kevo (Figure 5). On average, the daily contribution of mean T_{birch} to ET_{eco} reached peak values of *ca.* 65% in Abisko and *ca.* 30% in Kevo. However, the highly variable LAI in Abisko (Table 1) resulted in the upper bound of T_{birch}/ET_{eco} occasionally approaching 100% at this location (Figure 5c).

The value of T_{birch}/ET_{eco} increased with $\mathrm{VPD_{eco}}$ and $\mathrm{PAR_{eco}}$ (both log-transformed; Table S4, Figure 6a,b). In both cases, model selection retained the interaction between site and the environmental variable, but it was not significant for either driver (Table S4). We did not detect any effect of SMD on T_{birch}/ET_{eco} (Figure 6c; Table S4). We did not find any difference in T_{birch}/ET_{eco} between dry and wet days ($p = 0.27$).

The mean growing season contribution of T_{birch} to ET_{eco} was relatively low in Abisko (*ca.* 33%) but it was even lower in Kevo (16%, Table 4). Daily evapotranspiration by understorey components in Kevo was generally lower compared to T_{birch} (Figure 5d). For the whole of the growing season, $ET_{upscaled}$ only amounted to *ca.* 40% of ET_{eco} in Kevo (Table 4).

Daily ET_{eco} was higher in Abisko (Figure 5a,b), which also showed higher growing season totals compared to Kevo (Table 4). Remarkably, in Abisko ET_{eco} was 27% higher than the precipitation in the same period, while in Kevo the ecosystem returned to the atmosphere only *ca.* 59% of precipitation (ET_{eco}/P, Table 4). Nevertheless, the relative role of mountain birch transpiration in recycling precipitation was much higher in Abisko than in Kevo (T_{birch}/P, Table 4).

4. Discussion

4.1. Differences in seasonal and environmental controls on transpiration and evapotranspiration between sites

Boreal and arctic regions are undergoing very rapid and pronounced climatic warming, which is expected to modify water and energy fluxes across much of the terrestrial biosphere of these northern regions. We find that controls of evaporative fluxes by mixed birch-tundra communities of Northern Fennoscandia largely consist of controls by VPD (which strongly depends on air and canopy temperature) and by PAR. The relative importance of these effects depended partly on specific site conditions and the scale (branch versus ecosystem) at which they were considered. Predicted increases in air temperature can therefore be expected to increase the relative contribution of VPD relative to PAR in controlling evaporative fluxes.

Conversely, we find that the evaporative fluxes are not affected by temporal changes in soil moisture, suggesting that water supply is currently not a major limiting factor to evapotranspiration. Thus, there were no edaphic drought stress effects in T_{leaf} regulation by mountain birch, confirming results observed for other birch species (Gartner, Nadezhdina, Englisch, Čermak, & Leitgeb, 2009; Yan et al., 2018). Our results at the ecosystem level are consistent with field studies in forest-tundra systems (Beringer et al., 2005) and with a recent data synthesis, where no effect of soil moisture was reported for evapotranspiration at high latitudes (Kasurinen et al., 2014). Nevertheless, evaporative fluxes in boreal forests in more continental climates, with higher evaporative demands, may be influenced by soil moisture (Ohta et al., 2008).

At the seasonal time scale, fluxes were primarily controlled by LAI dynamics at both sites (cf. Poyatos et al., 2012). Seasonal courses of T_{leaf} and ET_{eco} mirrored each other, except during the start of the growing season in Abisko, when the discrepancy between T_{leaf} and ET_{eco} may have been caused by combined errors in the quantification of low fluxes and leaf area during early leaf development. Alternatively, this temporal mismatch between T_{leaf} and ET_{eco} may have been driven by substantial evaporation from moist soils after snowmelt and/or spatial variability in the phenology of greening up between the measured branches and the rest of the forest.

Both T_{leaf} and ET_{eco} were higher in Abisko than in Kevo because of the generally higher evaporative demand in Abisko (Figure 2). Environmental controls on T_{leaf} were very similar across sites. The only significant difference in the response of T_{leaf} to PAR may be due to differences in stand structure at the plot level (Table 1). The responses of evaporative fluxes to PAR and VPD differed between the two sites more clearly for T_{leaf} than for ET_{eco}, suggesting a higher sensitivity to VPD of the birch canopy compared to other ecosystem components (see also section 4.2). The negative interaction between VPD and PAR produced complex response surfaces of evaporative fluxes to environmental conditions. Model responses during conditions of high evaporative demand were reasonable, apart from those by ET_{eco} at Abisko, where the model showed a decrease of ET_{eco} with VPD at high PAR. The more extreme responses were found for unrealistic combinations of environmental conditions, which are not usually found in the field. (i.e. high VPD and low PAR), and when the model's predictions of the interaction effects are less reliable.

4.2. Contribution of mountain birch transpiration to ecosystem evapotranspiration across sites and environmental conditions

The mean daily contribution of birch transpiration to ecosystem evapotranspiration (i.e. T_{birch}/ET_{eco}) was much higher in Abisko than in Kevo. In Abisko, the higher variability in LAI at the landscape level propagates to a larger range of T_{birch}/ET_{eco} values compared to Kevo. When explaining seasonal variability in T_{birch}/ET_{eco}, we found that T_{birch}/ET_{eco} strongly depended on VPD and PAR, with T_{birch}/ET_{eco} saturating at high VPD, but this environmental control on T_{birch}/ET_{eco} was stronger in Abisko. Therefore, our results show an increased relative role of mountain birch in controlling ecosystem evapotranspiration as evaporative demand increases, especially in denser forests, in contrast with studies on waterlogged peatlands where understorey contribution increases with VPD (Ikawa et al., 2015). In our sites, mountain birch roots possibly access soil moisture at greater depths (Hunziker, Sigurdsson, Halldorsson, Schwanghart, & Kuhn, 2014), supplying water to meet the increasing evaporative demand and causing the increase in T_{birch}/ET_{eco}.

At the growing season level, birch transpiration contributed *ca.* 33% of total ecosystem evapotranspiration in Abisko but the contribution was only *ca.* 16% in Kevo (Table 4). These differences were attributable not only to a higher birch LAI in Abisko (Table 1), but also to the higher T_{leaf} values at this site (Figure 2). Lower T_{birch}/ET_{eco} values in Kevo could also result from a disproportionately higher contribution from the understorey in a sparser woodland (i.e. higher below-canopy incident radiation compared to Abisko). The values of of T_{birch}/ET_{eco} at the two sites are consistent with the generally low contribution of overstorey to total evapotranspiration in subarctic and northern boreal forests (Iida et al., 2009; Ikawa et al., 2015; Kelliher et al., 1997; Lafleur, 1992; Warren et al., 2019). However, in Kevo, our estimates of upscaled evapotranspiration from individual ecosystem components (i.e. mountain birch, understorey shrubs and lichen heath) yielded growing season values, which were still far from total ecosystem evapotranspiration measured by eddy covariance (Table 4, cf. section 4.3). In the following section, we discuss potential methodological artefacts and unmeasured processes that could explain this discrepancy.

4.3. Methodological considerations

This study jointly analyses a multi-scale dataset of evaporative fluxes from subarctic forest communities. Comparing evaporative fluxes across scales is hindered by the numerous potential errors associated with measurement techniques and upscaling procedures. Transpiration measurements from closed chambers could have been affected by radiation-driven overheating (Poyatos et al., 2012), by raising $\mathrm{VPD_{branch}}$ above $\mathrm{VPD_{eco}}$ and causing an overestimation of T_{leaf}. However, the relatively low values of T_{birch} and $ET_{upscaled}$, both based on closed chamber measurements, do not suggest that the conclusions of this study could have been affected by this artefact.

The upscaling procedure also has a number of potential limitations that warrant consideration. Due to the sparseness of the forest in Kevo (i.e. little shading effects on understorey vegetation), we assumed that the magnitude and regulation of understorey evapotranspiration was similar to that shown by patches with similar composition in the forest-tundra transition (Poyatos et al., 2014). However, LAI of the patches measured with automated chambers in the forest-mire transition (see section 2.5) was *ca.* 50% of the LAI actually measured in survey plots located within the forest (Table 1). Rescaling the understorey fluxes according to this understorey LAI, evapotranspiration from understorey components at the ecosystem level would be amount to 23.6 mm, an evaporative flux 55% larger than $T_{birch.}$ Scaling-up evapotranspiration estimated from canopy and understorey components, accounting for their land cover fractions and applying the LAI correction outlined above to understorey measurements would increase growing season $ET_{upscaled}$ values to 44.4 mm, or *ca.* 45% of ET_{eco}.

4.4. Differences in growing season water balance across sites

Even accounting for this likely underestimation of ET_{shrub} and ET_{lichen}, there is still a fraction of ET_{eco} that cannot be explained by upscaled gas exchange measurements from individual ecosystem components. Taking into account that T_{birch} obtained from branch-bag measurements excludes evaporation of intercepted water, we showed that T_{birch}/ET_{eco} does not vary between dry and wet days. This may suggest that evaporation of intercepted water may not be captured by eddy covariance measurements, otherwise T_{birch}/ET_{eco} would have been lower on wet days than dry days. Potentially high evaporation rates after precipitation may be partially missed from ET_{eco} and $ET_{upscaled}$, because data from open-path gas analysers are removed when the sensor windows are wet and subsequent gap-filling would not account for the missed evaporation of intercepted water (Oishi, Oren, & Stoy, 2008). Combined interception by overstorey canopies and mosses in northern boreal forests may amount up to 40% of bulk precipitation (Price, Dunham, Carleton, & Band, 1997), and we are not currently accounting for this substantial contribution.

We found stark differences between sites in the percentage of precipitation returned to the atmosphere as evapotranspiration; the mountain birch woodland in Abisko evaporated more water than it received during the growing season, as observed in other deciduous boreal forests (Blanken et al., 2001; Kelliher et al., 1997). In contrast, Kevo showed a substantial water surplus (Table 4). Our measurements did not include the snowmelt period, but these sites can reach snowpack depths of > 1 m (data for Kevo, 2009) and tree water uptake during this period, especially from deciduous species, can progressively deplete soil water sources (Young-Robertson et al., 2016). This decline in soil water content after snowmelt is very clear in the seasonal course of SMD measured in Abisko in 2008 and 2009 (outside our measurement period in Abisko, Fig S5). Therefore, these differences in the role of the mountain birch canopy between Abisko and Kevo, mediated by their different stand structure, can illustrate the potential changes in the hydrological regime that can result from the expansion and densification of subarctic deciduous woodlands.

4.5. Concluding remarks

We have shown that the dominant mountain birch canopy plays only a partial role in driving ecosystem evapotranspiration in both subarctic sites, and this may be a general feature of low-LAI subarctic and northern boreal forests (Saugier, Granier, Pontailler, Dufrene, & Baldocchi, 1997). Our results also show that both increased woodland cover and increased woodland density under climate change conditions (Rundqvist et al., 2011) will result in larger controls of the water fluxes by the canopies of deciduous trees as opposed to the understorey vegetation. However, our upscaling exercise also shows that adequately accounting for understorey components (and transpiration vs evaporation processes; Stoy et al., 2019) may be necessary to constrain future hydrological changes in these areas. The highly variable and patchy nature of subarctic vegetation may require flux upscaling approaches considering spatial variation not only of land cover (Hartley et al., 2015), but also of LAI (Stoy et al., 2013).

In the longer term, shifts towards deciduous-dominated communities in subarctic regions and an increased land cover by forest as opposed to tundra are expected to induce large hydro-climatic effects. These effects are expected to be mediated by higher transpiration rates, inducing complex land-climate feedbacks (Bonfils et al., 2012; Swann et al., 2010), which need to be considered together with carbon- and energy-related feedbacks (Wit et al., 2014). Overall, combining several flux datasets and land cover information we provide, for the poorly studied subarctic deciduous woodlands, highly valuable results that will help to calibrate and validate evapotranspiration processes in ecosystem models.

Acknowledgements

AM. Sabater is supported by European Social Fund and Generalitat Valenciana (GVA) under a PhD contract (ACIF – 2017/9830). This study was funded by the following grants: ABACUS NE/D005795/1 (NERC, UK), SAPFLUXNET CGL2014-JIN-55583 (MINECO, Spain), VERSUS CGL2015-67466-R (MINECO/FEDER), SGR-2017-1001 (AGAUR, Generalitat de Catalunya) and IMAGINA PROMETEU/2019/110 (Conselleria de Cultura, GVA). We are grateful for the support by the staff at the Kevo Subarctic Research Institute and at the Abisko Research Station. We would also like to acknowledge the help in the field by T. August, A. Robertson, K. Leslie, D. Sayer and J.R.M. Allen.

References

Aubinet, M., Vesala, T., & Papale, D. (2012). *Eddy Covariance: A Practical Guide to Measurement and Data Analysis*. Springer Science & Business Media.

Beringer, J., Chapin, F. S., Thompson, C. C., & McGuire, A. D. (2005). Surface energy exchanges along a tundra-forest transition and feedbacks to climate. *Agricultural and Forest Meteorology*, *131*(3–4), 143–161.

Blanken, P. D., Black, T. A., Neumann, H. H., den Hartog, G., Yang, P. C., Nesic, Z., & Lee, X. (2001). The seasonal water and energy exchange above and within a boreal aspen forest. *Journal of Hydrology*, *245*(1–4), 118–136. https://doi.org/10.1016/S0022-1694(01)00343-2

Bonan, G. B. (2008). Forests and Climate Change: Forcings, Feedbacks, and the Climate Benefits of Forests. *Science*, *320*, 1444–1449. https://doi.org/10.1126/science.1155121

Bonfils, C. J. W., Phillips, T. J., Lawrence, D. M., Cameron-Smith, P., Riley, W. J., & Subin, Z. M. (2012). On the influence of shrub height and expansion on northern high latitude climate. *Environmental Research Letters*, *7*(1), 015503. https://doi.org/10.1088/1748-9326/7/1/015503

Brümmer, C., Black, T. A., Jassal, R. S., Grant, N. J., Spittlehouse, D. L., Chen, B., … Wofsy, S. C. (2011). How climate and vegetation type influence evapotranspiration and water use efficiency in Canadian forest, peatland and grassland ecosystems. *Agricultural and Forest Meteorology*. https://doi.org/10.1016/j.agrformet.2011.04.008

Callaghan, T. V., Björn, L. O., Chapin Iii, F., Chernov, Y., Christensen, T. R., Huntley, B., … Shaver, G. R. (2005). Arctic tundra and polar desert ecosystems. In *Arctic climate impact assessment* (Vol. 1, pp. 243–352).

Callaghan, T. V., Jonasson, C., Thierfelder, T., Yang, Z., Hedenås, H., Johansson, M., … Sloan, V. L. (2013). Ecosystem change and stability over multiple decades in the Swedish subarctic: Complex processes and multiple drivers. *Philosophical Transactions of the Royal Society B: Biological Sciences*, *368*(1624), 20120488. https://doi.org/10.1098/rstb.2012.0488

Chapin, F. S., Mcguire, A. D., Randerson, J., Pielke, R., Baldocchi, D., Hobbie, S. E., … Running, S. W. (2000). Arctic and boreal ecosystems of western North America as components of the climate system. *Global Change Biology*, *6*(S1), 211–223. https://doi.org/10.1046/j.1365-2486.2000.06022.x

Cohen, L. R., Raz-Yaseef, N., Curtis, J. B., Young, J. M., Rahn, T. A., Wilson, C. J., … Newman, B. D. (2015). Measuring diurnal cycles of evapotranspiration in the Arctic with an automated chamber system. *Ecohydrology*, *8*(4), 652–659. https://doi.org/10.1002/eco.1532

Dahlberg, U., Berge, T. W., Petersson, H., & Vencatasawmy, C. P. (2004). Modelling biomass and leaf area index in a sub-arctic Scandinavian mountain area. *Scandinavian Journal of Forest Research*, *19*, 60–71. https://doi.org/10.1080/02827580310019266

Fletcher, B. J., Gornall, J. L., Poyatos, R., Press, M. C., Stoy, P. C., Huntley, B., … Phoenix, G. K. (2012). Photosynthesis and productivity in heterogeneous arctic tundra: Consequences for ecosystem function of mixing vegetation types at stand edges. *Journal of Ecology*, *100*(2), 441–451. https://doi.org/10.1111/j.1365-2745.2011.01913.x

Gartner, K., Nadezhdina, N., Englisch, M., Čermak, J., & Leitgeb, E. (2009). Sap flow of birch and Norway spruce during the European heat and drought in summer 2003. *Forest Ecology and Management*, *258*(5), 590–599. https://doi.org/10.1016/j.foreco.2009.04.028

Gash, J. H. C., & Dolman, A. J. (2003). Sonic anemometer (co)sine response and flux measurement: I. The potential for (co)sine error to affect sonic anemometer-based flux measurements. *Agricultural and Forest Meteorology*, *119*(3), 195–207. https://doi.org/10.1016/S0168-1923(03)00137-0

Granier, A., & Loustau, D. (1994). Measuring and modelling the transpiration of a maritime pine canopy from sap-flow data. *Agricultural and Forest Meteorology*, *71*, 61–81.

Grelle, A., Lundberg, A., Lindroth, A., Morén, A.-S., & Cienciala, E. (1997). Evaporation components of a boreal forest: Variations during the growing season. *Journal of Hydrology*, *197*(1), 70–87. https://doi.org/10.1016/S0022-1694(96)03267-2

Haapanala, S., Ekberg, A., Hakola, H., Tarvainen, V., Rinne, J., Hellén, H., & Arneth, A. (2009). Mountain birch–potentially large source of sesquiterpenes into high latitude atmosphere. *Biogeosciences*, *6*, 2709–2718.

Hartley, I. P., Hopkins, D. W., Sommerkorn, M., & Wookey, P. A. (2010). The response of organic matter mineralisation to nutrient and substrate additions in sub-arctic soils. *Soil Biology and Biochemistry*, *42*(1), 92–100.

Hartley, Iain. P., Hill, Timothy. C., Wade, Thomas. J., Clement, Robert. J., Moncrieff, John. B., Prieto-Blanco, Ana., … Baxter, Robert. (2015). Quantifying landscape-level methane fluxes in subarctic Finland using a multiscale approach. *Global Change Biology*, *21*(10), 3712–3725. https://doi.org/10.1111/gcb.12975

Hofgaard, A., Tømmervik, H., Rees, G., & Hanssen, F. (2013). Latitudinal forest advance in northernmost Norway since the early 20th century. *Journal of Biogeography*, *40*(5), 938–949. https://doi.org/10.1111/jbi.12053

Hunziker, M., Sigurdsson, B. D., Halldorsson, G., Schwanghart, W., & Kuhn, N. (2014). Biomass allometries and coarse root biomass distribution of mountain birch in southern Iceland. *Icelandic Agricultural Sciences*, *27*, 111–125.

Iida, S., Ohta, T., Matsumoto, K., Nakai, T., Kuwada, T., Kononov, A. V., … Yabuki, H. (2009). Evapotranspiration from understory vegetation in an eastern Siberian boreal larch forest. *Agricultural and Forest Meteorology*, *149*(6), 1129–1139. https://doi.org/10.1016/j.agrformet.2009.02.003

Ikawa, H., Nakai, T., Busey, R. C., Kim, Y., Kobayashi, H., Nagai, S., … Hinzman, L. (2015). Understory CO2, sensible heat, and latent heat fluxes in a black spruce forest in interior Alaska. *Agricultural and Forest Meteorology*, *214–215*, 80–90. https://doi.org/10.1016/j.agrformet.2015.08.247

IPCC. (2013). *Climate Change 2013: The Physical Science Basis. Contribution of Working Group I to the Fifth Assessment Report of the Intergovernmental Panel on Climate Change*. https://doi.org/10.1017/CBO9781107415324

Kasurinen, V., Alfredsen, K., Kolari, P., Mammarella, I., Alekseychik, P., Rinne, J., … Berninger, F. (2014). Latent heat exchange in the boreal and arctic biomes. *Global Change Biology*, *20*(11), 3439–3456. https://doi.org/10.1111/gcb.12640

Kattsov, V. M., Källén, E., Cattle, H. P., Christensen, J., Drange, H., Hanssen-Bauer, I., … others. (2005). *Future climate change: Modeling and scenarios for the Arctic*.

Kelliher, F. M., Hollinger, D. Y., Schulze, E.-D., Vygodskaya, N. N., Byers, J. N., Hunt, J. E., … Bauer, G. (1997). Evaporation from an eastern Siberian larch forest. *Agricultural and Forest Meteorology*, *85*(3), 135–147. https://doi.org/10.1016/S0168-1923(96)02424-0

Knauer, J., Werner, C., & Zaehle, S. (2015). Evaluating stomatal models and their atmospheric drought response in a land surface scheme: A multibiome analysis. *Journal of Geophysical Research: Biogeosciences*, *120*(10), 2015JG003114. https://doi.org/10.1002/2015JG003114

Krankina, O. N., Pflugmacher, D., Hayes, D. J., McGuire, A. D., Hansen, M. C., Häme, T., … Nelson, P. (2010). Vegetation cover in the eurasian arctic: Distribution, monitoring, and role in carbon cycling. In *Eurasian arctic land cover and land use in a changing climate* (pp. 79–108). Springer.

Lafleur, P. M. (1992). Energy balance and evapotranspiration from a subarctic forest. *Agricultural and Forest Meteorology*, *58*(3–4), 163–175. https://doi.org/10.1016/0168-1923(92)90059-D

McFadden, J. P., Eugster, W., & Chapin III, F. S. (2003). A regional study of the controls on water vapor and CO2 exchange in arctic tundra. *Ecology*, *84*(10), 2762–2776.

Mekonnen, Z. A., Riley, W. J., Randerson, J. T., Grant, R. F., & Rogers, B. M. (2019). Expansion of high-latitude deciduous forests driven by interactions between climate warming and fire. *Nature Plants*, 1–7. https://doi.org/10.1038/s41477-019-0495-8

Myers-Smith, I. H., Forbes, B. C., Wilmking, M., Hallinger, M., Lantz, T., Blok, D., … Hik, D. S. (2011). Shrub expansion in tundra ecosystems: Dynamics, impacts and research priorities. *Environmental Research Letters*, *6*(4), 045509. https://doi.org/10.1088/1748-9326/6/4/045509

Nakagawa, S., & Schielzeth, H. (2013). A general and simple method for obtaining R2 from generalized linear mixed-effects models. *Methods in Ecology and Evolution*, *4*(2), 133–142. https://doi.org/10.1111/j.2041-210x.2012.00261.x

Nyström, M., Holmgren, J., & Olsson, H. (2012). Prediction of tree biomass in the forest–tundra ecotone using airborne laser scanning. *Remote Sensing of Environment*, *123*, 271–279. https://doi.org/10.1016/j.rse.2012.03.008

Ohta, T., Maximov, T. C., Dolman, A. J., Nakai, T., van der Molen, M. K., Kononov, A. V., … Yabuki, H. (2008). Interannual variation of water balance and summer evapotranspiration in an eastern Siberian larch forest over a 7-year period (1998–2006). *Agricultural and Forest Meteorology*, *148*(12), 1941–1953. https://doi.org/10.1016/j.agrformet.2008.04.012

Oishi, A. C., Oren, R., & Stoy, P. C. (2008). Estimating components of forest evapotranspiration: A footprint approach for scaling sap flux measurements. *Agricultural and Forest Meteorology*, *148*(11), 1719–1732.

Pinheiro, J., Bates, D., DebRoy, S., Sarkar, D., & R Core Team. (2018). *nlme: Linear and Nonlinear Mixed Effects Models*. Retrieved from https://CRAN.R-project.org/package=nlme

Poyatos, R., Gornall, J., Mencuccini, M., Huntley, B., & Baxter, R. (2012). Seasonal controls on net branch CO2 assimilation in sub-Arctic Mountain Birch (Betula pubescens ssp. Czerepanovii (Orlova) Hamet-Ahti). *Agricultural and Forest Meteorology*, *158–159*, 90–100. https://doi.org/10.1016/j.agrformet.2012.02.009

Poyatos, R., Heinemeyer, A., Ineson, P., Evans, J. G., Ward, H. C., Huntley, B., & Baxter, R. (2014). Environmental and Vegetation Drivers of Seasonal CO2 Fluxes in a Sub-arctic Forest–Mire Ecotone. *Ecosystems*, *17*(3), 377–393. https://doi.org/10.1007/s10021-013-9728-2

Price, A. G., Dunham, K., Carleton, T., & Band, L. (1997). Variability of water fluxes through the black spruce (Picea mariana) canopy and feather moss (Pleurozium schreberi) carpet in the boreal forest of Northern Manitoba. *Journal of Hydrology*, *196*(1), 310–323. https://doi.org/10.1016/S0022-1694(96)03233-7

Rayment, M. B., & Jarvis, P. G. (1999). Seasonal gas exchange of black spruce using an automatic branch bag system. *Canadian Journal of Forest Research*, *29*, 1528–1538.

Rundqvist, S., Hedenås, H., Sandström, A., Emanuelsson, U., Eriksson, H., Jonasson, C., & Callaghan, T. V. (2011). Tree and Shrub Expansion Over the Past 34 Years at the Tree-Line Near Abisko, Sweden. *AMBIO: A Journal of the Human Environment*, *40*(6), 683–692. https://doi.org/10.1007/s13280-011-0174-0

Saugier, B., Granier, A., Pontailler, J. Y., Dufrene, E., & Baldocchi, D. D. (1997). Transpiration of a boreal pine forest measured by branch bag, sap flow and micrometeorological methods. *Tree Physiology*, *17*, 511–519.

Schlesinger, W. H., & Jasechko, S. (2014). Transpiration in the global water cycle. *Agricultural and Forest Meteorology*, *189–190*, 115–117. https://doi.org/10.1016/j.agrformet.2014.01.011

Schotanus, P., Nieuwstadt, F. T. M., & De Bruin, H. A. R. (1983). Temperature measurement with a sonic anemometer and its application to heat and moisture fluxes. *Boundary-Layer Meteorology*, *26*(1), 81–93. https://doi.org/10.1007/BF00164332

Stoy, P. C., Williams, M., Evans, J. G., Prieto-Blanco, A., Disney, M., Hill, T. C., … Street, L. E. (2013). Upscaling tundra CO_2 exchange from chamber to eddy covariance tower. *Arctic, Antarctic, and Alpine Research*, *45*(2), 275–284.

Stoy, Paul C., El-Madany, T. S., Fisher, J. B., Gentine, P., Gerken, T., Good, S. P., … Wolf, S. (2019). Reviews and syntheses: Turning the challenges of partitioning ecosystem evaporation and transpiration into opportunities. *Biogeosciences*, *16*(19), 3747–3775. https://doi.org/10.5194/bg-16-3747-2019

Stoy, Paul C., Mauder, M., Foken, T., Marcolla, B., Boegh, E., Ibrom, A., … Varlagin, A. (2013). A data-driven analysis of energy balance closure across FLUXNET research sites: The role of landscape scale heterogeneity. *Agricultural and Forest Meteorology*, *171–172*, 137–152. https://doi.org/10.1016/j.agrformet.2012.11.004

Swann, A. L., Fung, I. Y., Levis, S., Bonan, G. B., & Doney, S. C. (2010). Changes in Arctic vegetation amplify high-latitude warming through the greenhouse effect. *Proceedings of the National Academy of Sciences*, *107*(4), 1295–1300. https://doi.org/10.1073/pnas.0913846107

Tømmervik, H., Johansen, B., Tombre, I., Thannheiser, D., Høgda, K. A., Gaare, E., & Wielgolaski, F. E. (2004). Vegetation Changes in the Nordic Mountain Birch Forest: The Influence of Grazing and Climate Change. *Arctic, Antarctic, and Alpine Research*, *36*(3), 323–332.

Wang, J. A., Sulla-Menashe, D., Woodcock, C. E., Sonnentag, O., Keeling, R. F., & Friedl, M. A. (2019). Extensive land cover change across Arctic–Boreal Northwestern North America from disturbance and climate forcing. *Global Change Biology*, *0*(0). https://doi.org/10.1111/gcb.14804

Warren, R. K., Pappas, C., Helbig, M., Chasmer, L. E., Berg, A. A., Baltzer, J. L., … Sonnentag, O. (2019). Minor contribution of overstorey transpiration to landscape evapotranspiration in boreal permafrost peatlands. *Ecohydrology*, *11*(5), e1975. https://doi.org/10.1002/eco.1975

Webb, E. K., Pearman, G. I., & Leuning, R. (1980). Correction of flux measurements for density effects due to heat and water vapour transfer. *Quarterly Journal of the Royal Meteorological Society*, *106*(447), 85–100. https://doi.org/10.1002/qj.49710644707

Welp, L. R., Randerson, J. T., & Liu, H. P. (2007). The sensitivity of carbon fluxes to spring warming and summer drought depends on plant functional type in boreal forest ecosystems. *Agricultural & Forest Meteorology*, *147*(3–4), 172–185.

Wingate, L., Seibt, U., Moncrieff, J. B., Jarvis, P. G., & Lloyd, J. (2007). Variations in13C discrimination during CO2 exchange by Picea sitchensis branches in the field. *Plant, Cell & Environment*, *30*(5), 600–616. https://doi.org/10.1111/j.1365-3040.2007.01647.x

Wit, H. A. de, Bryn, A., Hofgaard, A., Karstensen, J., Kvalevåg, M. M., & Peters, G. P. (2014). Climate warming feedback from mountain birch forest expansion:

Reduced albedo dominates carbon uptake. *Global Change Biology*, *20*(7), 2344–2355. https://doi.org/10.1111/gcb.12483

Yan, C., Wang, B., Zhang, Y., Zhang, X., Takeuchi, S., & Qiu, G. (2018). Responses of Sap Flow of Deciduous and Conifer Trees to Soil Drying in a Subalpine Forest. *Forests*, *9*(1), 32. https://doi.org/10.3390/f9010032

Young-Robertson, J. M., Bolton, W. R., Bhatt, U. S., Cristóbal, J., & Thoman, R. (2016). Deciduous trees are a large and overlooked sink for snowmelt water in the boreal forest. *Scientific Reports*, *6*, srep29504. https://doi.org/10.1038/srep29504

Zhang, W., Miller, P. A., Smith, B., Wania, R., Koenigk, T., & Döscher, R. (2013). Tundra shrubification and tree-line advance amplify arctic climate warming: Results from an individual-based dynamic vegetation model. *Environmental Research Letters*, *8*(3), 034023. https://doi.org/10.1088/1748-9326/8/3/034023

Zuur, A. F., Ieno, E. N., & Elphick, C. S. (2010). A protocol for data exploration to avoid common statistical problems. *Methods in Ecology and Evolution*, *1*(1), 3–14. https://doi.org/10.1111/j.2041-210X.2009.00001.x

Tables

Table 1. Stand characteristics of mountain birch forests in Abisko and Kevo. Values labelled as 'Site' represent the site mean (±SE) of all inventory plots in Abisko (N=6) and Kevo (N=8). Values labelled as 'BB' are the values of the plots in the vicinity of the branch bags measuring sites. Tree density refers to polycormic individuals, with multiple stems per tree.

	Tree density (trees ha^{-1})	Stems per tree	Basal area ($m^2 ha^{-1}$)	DBH (mm)	Height (m)	Overstorey LAI_{max} (m^2 m^{-2})	Understorey LAI_{max} (m^2 m^{-2})
Abisko							
Site	1260 ± 80	3.7 ± 0.2	6.5 ± 0.2	36.9 ± 1.0	3.9 ± 0.2	1.2 ± 0.3	1.0 ± 0.2
BB	1146	4.4	6.7	35.7	-	1.8	-
Kevo							
Site	876 ± 85	3.3 ± 0.2	3.8 ± 0.4	37. 2 ± 2.0	3.8 ± 0.0	0.7 ± 0.1	1.5 ± 0.1
BB	833	3.8	3.0	30.6	3.8	0.6	-

Table 2. Summary statistics of the linear mixed model of log-transformed T_{leaf} as a function of environmental variables ($\text{VPD}_{\text{branch}}$, $\text{PAR}_{\text{branch}}$ and SMD) for Abisko and Kevo. Asterisks denote significant differences from zero ($^{*}p<0.05$, $^{**}p<0.01$, $^{***}p<0.001$). Statistical differences in model coefficients ($p < 0.05$) between Abisko and Kevo were marked in bold. SD: Standard deviation. Interactions between variables are denoted by colon (:) and variables not included after model selection are denoted by 'n.i'.

	Abisko	Kevo
Fixed effects		
Intercept	**$-2.98 \pm 0.09^{*}$**	**$-4.00 \pm 0.07^{***}$**
$\log(\text{VPD}_{\text{branch}})$	$1.26 \pm 0.01^{***}$	$1.27 \pm 0.01^{***}$
$\text{PAR}_{\text{branch}}$	**$4.1\cdot10^{-4} \pm 0.4\cdot10^{-4***}$**	**$7.5\cdot10^{-4} \pm 0.4\cdot10^{-4***}$**
$\log(\text{VPD}_{\text{branch}})$: $\text{PAR}_{\text{branch}}$	$-8.4\cdot10^{-4} \pm 0.5\cdot10^{-4***}$	$-9.4\cdot10^{-4} \pm 0.4\cdot10^{-4***}$
SMD	n.i.	n.i.
Random effects (branch)		
SD (Intercept)	0.26	0.20
Residual error	0.40	0.48
Correlation structure (φ)	$4.40\cdot10^{-8}$	$7.23\cdot10^{-7}$
R^2 marginal (R^2 conditional)	0.78 (0.84)	0.77 (0.80)

Table 3. Summary statistics of the generalised least squares model of ET_{eco} as a function of environmental variables (VPD_{eco}, PAR_{eco} and SMD) for Abisko and Kevo. Asterisks denote significant differences from zero ($^{*}p<0.05$, $^{**}p<0.01$, $^{***}p<0.001$). No significant differences ($p < 0.05$) were found between model coefficients between Abisko and Kevo. Interactions between variables are denoted by colon (:) and variables not included after model selection are denoted by 'n.i'.

	Abisko	Kevo
Intercept	$-4.93 \pm 0.38^{***}$	$-4.84 \pm 0.40^{***}$
log(VPD)	$2.58 \pm 0.30^{***}$	$2.13 \pm 0.27^{***}$
$\log(PAR_{eco})$	$0.47 \pm 0.06^{***}$	$0.47 \pm 0.06^{***}$
$\log(VPD_{eco}):\log(PAR_{eco})$	$-0.39 \pm 0.05^{***}$	$-0.26 \pm 0.05^{***}$
SMD	n.i.	n.i.
Correlation structure (φ)	$8.23 \cdot 10^{-3}$	$1.84 \cdot 10^{-2}$
R^2 marginal	0.71	0.69

Table 4. Growing season values of precipitation (P), birch transpiration (T_{birch}) and ecosystem evapotranspiration (ET_{eco}) in Abisko and Kevo. Percentage of evaporative fluxes as a fraction of ET_{eco} and P are also shown for growing season values. Values with an uncertainty measure represent means ± standard error.

	Abisko	Kevo
T_{birch} (mm)	52.5 ± 13.0	15.2 ± 1.5
ET_{eco} (mm)	160.5	98.5
$ET_{upscaled}$ (mm)	-	39.4 ± 1.5
T_{birch} / ET_{eco} (%)	32.7 ± 8.1	15.5 ± 1.5
T_{birch} / P (%)	41.4 ± 10.2	9.1 ± 0.9
ET_{eco} / P (%)	126.6	58.8
$ET_{upscaled}$ / ET_{eco} (%)	-	40.0 ± 1.5

Figure captions

Figure 1. Study sites at Abisko (a) and Kevo (b), showing the locations of the branch bags systems, the eddy flux towers and the understorey automated chambers at Kevo. Panel (a) shows the aerial photography obtained in Abisko and (b) shows the land classification at Kevo obtained from aerial photography (cf. Hartley et al., 2015). *Birch* : mountain birch woodland; *Understorey*: low- and dwarf-shrubs; *Lichen*: lichen heath; *Mire*: organic hummocks and interhummocks with shrubs and *Spahgnum*; *Water*: open water; *Lawns*: graminoid lawns; *Board*: boardwalks; *Other*: other land cover.

Figure 2. Seasonal course of environmental variables and evaporative fluxes (daily means) in Abisko and Kevo. Environmental variables include photosynthetically active radiation (a-b, PAR), vapour pressure deficit (c-d, VPD) and rainfall (e, f). Environmental variables were measured at the ecosystem (black lines) and at the branch level (red lines). Mountain birch transpiration per unit leaf area (g-h, T_{eaf}) and ecosystem evapotranspiration (i-j, ET_{eco}) are also shown. Standard error is shown as shaded grey.

Figure 3. Sub-daily responses of ecosystem evapotranspiration (ET_{eco}) and mountain birch transpiration per unit leaf area (T_{eaf}) to PAR (panels a,c) and VPD (panels b,d), measured at the corresponding ecological scale (i.e. 'branch' for T_{leaf} and 'eco' for ET_{eco}) in Abisko (red) and Kevo (blue).

Figure 4. Response surfaces of modelled T_{leaf} (panels a, b) and ET_{eco} (panels c, d) as a function of VPD and PAR, in Abisko (panels a, c) and Kevo (panels b, d). Please note the different scales in the VPD axes in panels a and b compared to panels c and d.

Figure 5. Seasonal course of daily ecosystem evapotranspiration (ET_{eco}, black lines) and upscaled birch transpiration (T_{birch}, grey lines), for Abisko (a) and Kevo (b). The shaded regions in panels a and b depict upscaled T_{birch} using mean±SE values of LAI (Table 1). Daily percentage of T_{birch}/ET_{eco} for Abisko (c) and Kevo (d). Panel (f) shows evapotranspiration components and their upscaled values for Kevo only: ET_{eco} (black line), T_{birch} (grey line), ET_{shrub} (purple line), ET_{lichen} (green line), $ET_{upscaled}$ (asterisk).

Figure 6. Variation of daily T_{birch} / ET_{eco} in response to VPD_{eco} (a), PAR_{eco} (b) and SMD (c), for Abisko (red) and Kevo (blue). Models summary are shown in Table S3.

597 Significant interaction between site and environmental value is shown in solid line and
598 no-significant interaction in dashed line.

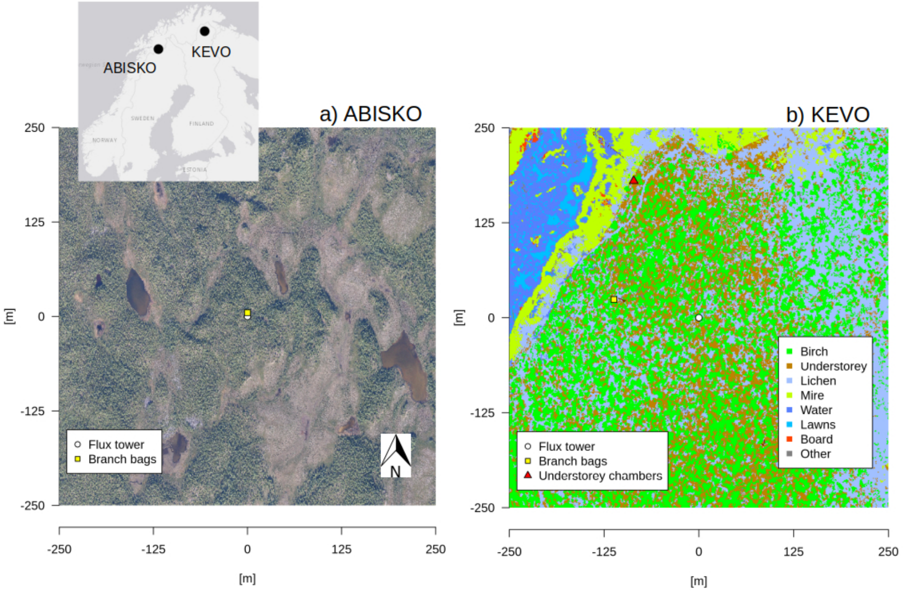

Figure 1. Study sites at Abisko (a) and Kevo (b), showing the locations of the branch bags systems, the eddy flux towers and the understorey automated chambers at Kevo. Panel (a) shows the aerial photography obtained in Abisko and (b) shows the land classification at Kevo obtained from aerial photography (cf. Hartley et al., 2015). Birch : mountain birch woodland; Understorey: low- and dwarf-shrubs; Lichen: lichen heath; Mire: organic hummocks and interhummocks with shrubs and Spahgnum; Water: open water; Lawns: graminoid lawns; Board: boardwalks; Other: other land cover.

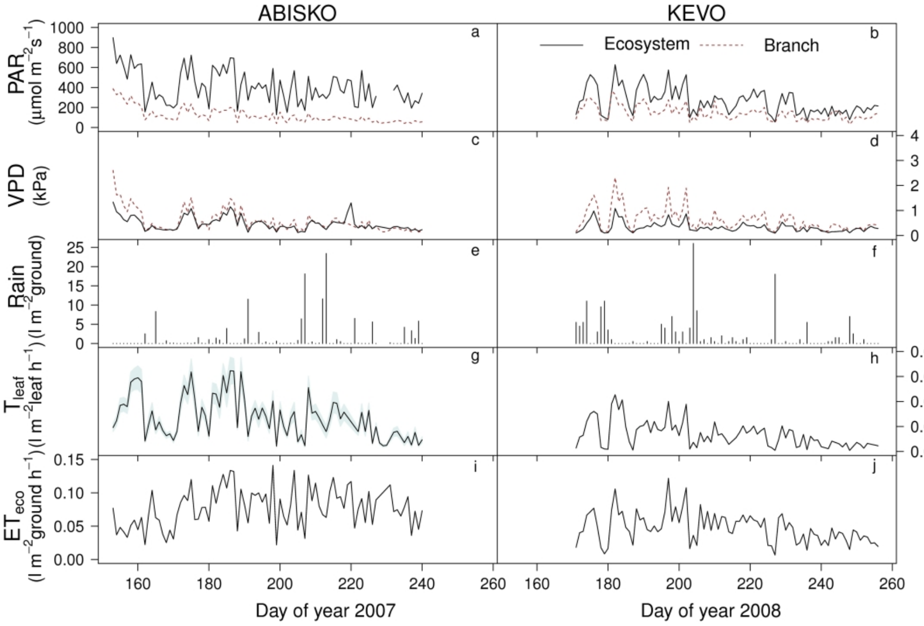

Figure 2. Seasonal course of environmental variables and evaporative fluxes (daily means) in Abisko and Kevo. Environmental variables include photosynthetically active radiation (a-b, PAR), vapour pressure deficit (c-d, VPD) and rainfall (e, f). Environmental variables were measured at the ecosystem (black lines) and at the branch level (red lines). Mountain birch transpiration per unit leaf area (g-h, Teaf) and ecosystem evapotranspiration (i-j, ETeco) are also shown. Standard error is shown as shaded grey.

359x242mm (300 x 300 DPI)

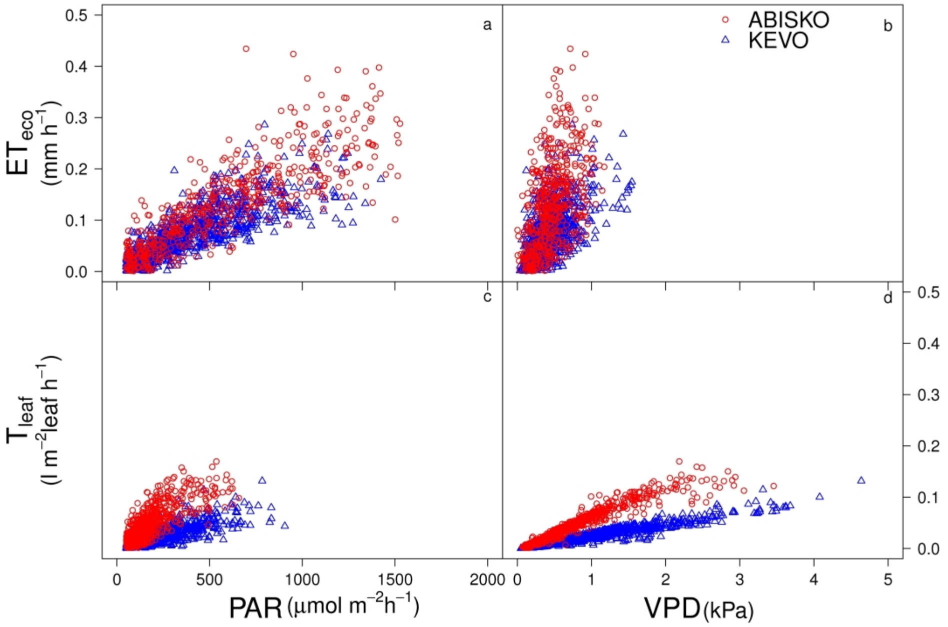

Figure 3. Sub-daily responses of ecosystem evapotranspiration (ETeco) and mountain birch transpiration per unit leaf area (Teaf) to PAR (panels a,c) and VPD (panels b,d), measured at the corresponding ecological scale (i.e. 'branch' for Tleaf and 'eco' for ETeco) in Abisko (red) and Kevo (blue).

349x242mm (300 x 300 DPI)

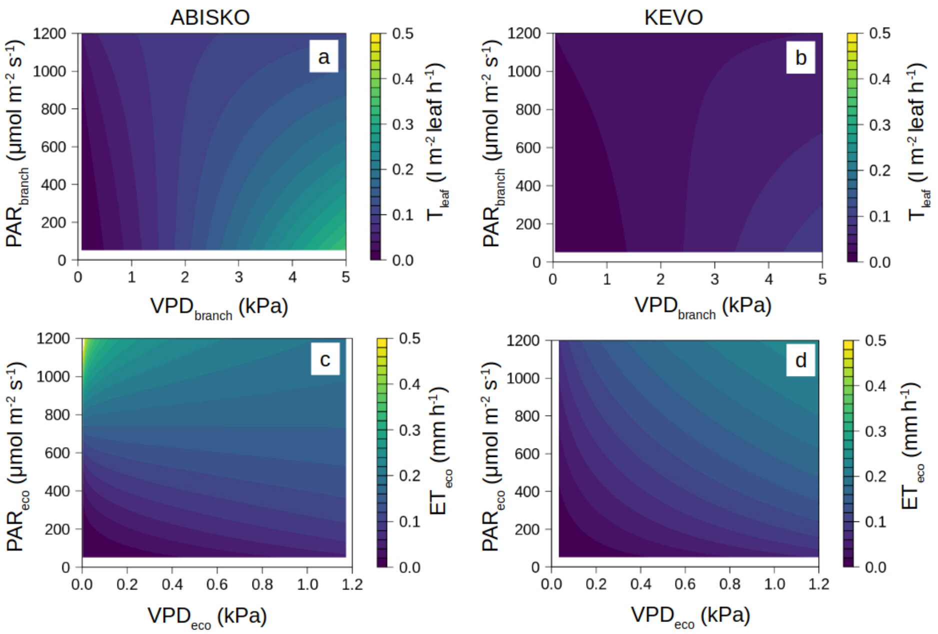

Figure 4. Response surfaces of modelled Tleaf (panels a, b) and ETeco (panels c, d) as a function of VPD and PAR, in Abisko (panels a, c) and Kevo (panels b, d). Please note the different scales in the VPD axes in panels a and b compared to panels c and d.

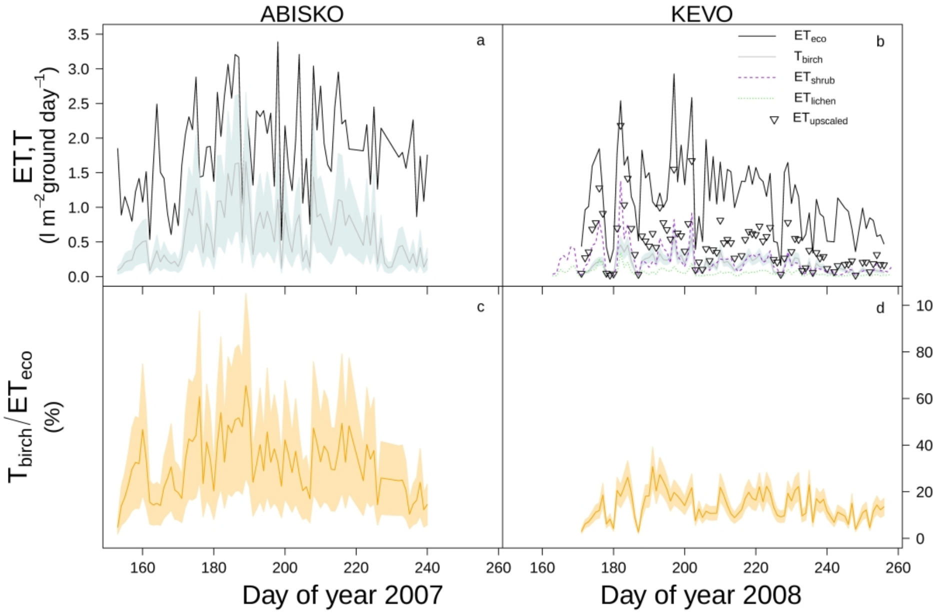

Figure 5. Seasonal course of daily ecosystem evapotranspiration (ETeco, black lines) and upscaled birch transpiration (Tbirch, grey lines), for Abisko (a) and Kevo (b). The shaded regions in panels a and b depict upscaled Tbirch using mean±SE values of LAI (Table 1). Daily percentage of Tbirch/ETeco for Abisko (c) and Kevo (d). Panel (f) shows evapotranspiration components and their upscaled values for Kevo only: ETeco (black line), Tbirch (grey line), ETshrub (purple line), ETlichen (green line), ETupscaled (asterisk).

370x242mm (300 x 300 DPI)

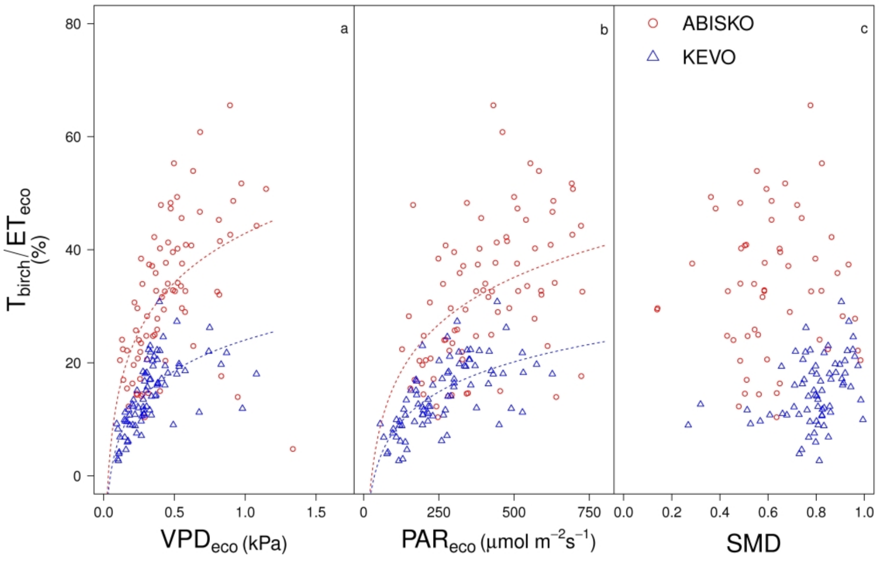

Figure 6. Variation of daily Tbirch / ETeco in response to VPDeco (a), PAReco (b) and SMD (c), for Abisko (red) and Kevo (blue). Models summary are shown in Table S3. Significant interaction between site and environmental value is shown in solid line and no-significant interaction in dashed line.

396x242mm (300 x 300 DPI)

Supporting Information

S1. Allometric relationships

Table S1. Summary statistics for the allometric relationships used to predict leaf area supported by individual stems in Abisko and Kevo. Intercepts are labelled as *a* and coefficients associated to the different predictors are labelled as b_i.

Site	Response [units]	a	SE	Predictor [units]	b_i	SE	R^2_{adj}
Abisko	ln(leaf biomass) [kg]	-8.11	0.71	ln (stem basal area) [mm^2]	0.43	0.11	0.86
				ln (stem height) [dm]	1.06	0.37	
Kevo	ln (leaf biomass) [g]	-4.95	0.25	ln (stem diameter) [mm]	1.56	0.07	0.97

In Kevo, trees frequently presented a number of small stems (DBH<12mm), whose number was recorded in the forest inventories; there were *ca.* 876 small stems ha^{-1}. To account for the leaf area supported by these stems, we assumed a typical diameter of 6 mm (half the value of the DBH threshold in the inventory) for these stems and applied the allometric relationship above. Leaf area of small stems amounted, on average, 5% of total plot leaf area.

S2. Technical description of the branch bags system

Branch bags (average volume=0.11 m^3) were hung from tripods and poles to enclose the sampled branches. A data-logger (CR10X, Campbell Scientific UK, Shepshed, Leicester, UK) and a control interface (SDM-CD16AC, Campbell Scientific UK) controlled which bag was being sampled by delivering power to the electromagnetic catch that sealed the bag, the internal mixing fan and the corresponding diaphragm pump. This pump sampled air from the bag (5 dm^3 min^{-1}) through polyethylene-lined tubing, 5 mm in diameter, to an enclosure where a solenoid and another pump diverted the air sample (0.2 dm^3 min^{-1}) to an IRGA (LI-6262, LICOR Inc., Lincoln NE, USA).

All the sampled branches were within *ca.* 10 m from this control box. Outputs from all sensors and IRGA were transmitted through a relay multiplexer (AM416, Campbell Scientific UK) and stored in the data-logger.

Each bag remained closed for 7.5 minutes (completing a measurement cycle of the eight branches in one hour), during which H_2O concentrations were measured every 5 s. with the IRGA operating in absolute mode. Air temperature, relative humidity (HMP45C, Vaisala, Vantaa, Finland), and air pressure (LI-6262-03, LI-COR Inc.) were also recorded every 5 s. Average Photosynthetically Active Radiation (PAR) was also measured inside the branch bags (SD101QV/SD201QV, Macam Ltd., Livingston, UK).

We calculated branch transpiration within the branch bag, T_{branch} (mmol s^{-1}), as:

$$E_{branch} = \frac{P_{bag}\,V_{bag}\,d}{RT_{bag,0}\;dt}[H_2O]_{bag} \qquad \text{(Eq. S1)}$$

Where P_{bag} (Pa) is air pressure, V_{bag} (m^3) is bag volume, R (J mol^{-1} K^{-1}) is the ideal gas constant, $T_{bag,0}$ (K) is absolute temperature inside the bag and $d[H_2O]_{bag}/dt$ (mmol s^{-1})is the rate of change in H_2O vapour concentration (mmol)during each observation. The $d[H_2O]_{bag}/dt$ (mmol s^{-1}) was estimated from the first order term of a quadratic fit between H_2O vapour concentration (mmol) and time since chamber closure (Poyatos, Gornall, Mencuccini, Huntley, & Baxter, 2012). Nonlinear fits describe better the concentration dynamics, and do not systematically underestimate the fluxes (Wagner, Reicosky, & Alessi, 1997). However, in the presence of noisy concentration data under low flux conditions, we opted for the more stable linear fit. We achieved this by selecting the linear regression whenever the slope for the linear fit and the linear term of the quadratic fit had opposite signs. Flux calculations were implemented in a R script (v 2.9, R Development Core Team, Vienna, Austria), which also included tests for autocorrelation (Durbin-Watson) and normality (Shapiro-Wilk) of residuals for each flux observation (Kutzbach et al., 2007), and produced diagnostic plots of instantaneousH_2O concentrations during each observation. The values of T_{branch} were transformed from molar to volume using the molar volume of water and converted to hourly rates (l $hour^{-1}$), prior to their conversion to transpiration per unit leaf area T_{leaf} (cf. main text).

S3.Energy balance closure in eddy covariance measurements

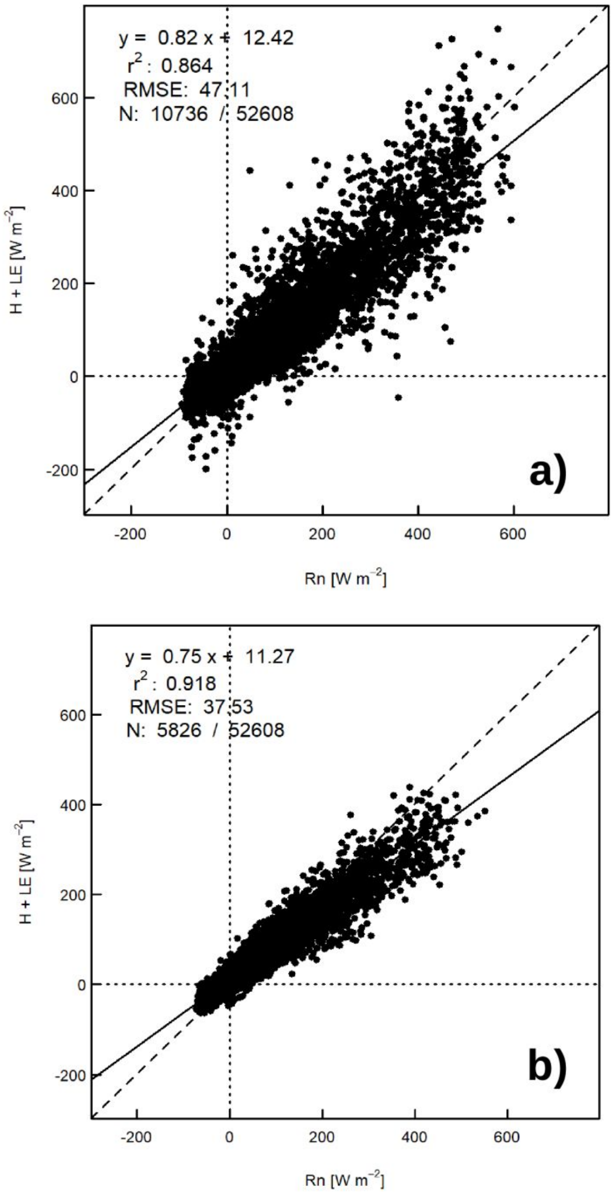

Figure S1. The sum of sensible and latent heat fluxes versus net radiation (ground heat flux and heat stored in the canopy are neglected) in Abisko (a) and Kevo (b).

56

S4. Data temporal aggregation and gap-filling

Due to technical problems of the measurement systems, gaps in temporal series were present. Not accounting for these gaps could bias the quantification of daily and seasonal aggregates of evaporative fluxes. To address this, hourly T_{leaf} and ET_{eco} were gap-filled with values predicted by the models presented in the main text (Table 2, 3). Gap-filling of ET_{shrub} and ET_{lichen} were performed using a similar modelling strategy, using PAR and VPD as predictors. The models for these two hourly fluxes showed a marginal and conditional R^2 of 0.54 and 0.56, respectively. However, we could not make predictions when meteorological variables were also missing. Therefore, daily aggregates of T_{leaf} were calculated when data for at least three branches and 50% of hours in each day were present; the same criterion for the minimum number of timesteps was applied for ET_{eco} and for environmental drivers such as PAR and VPD. Precipitation was calculated as the daily summation of hourly values. After this hourly gap-filling, days with missing data were imputed using daily models of the corresponding evaporative flux and its drivers. When drivers (VPD, PAR) were also missing, we gap-filledthese data using data from nearby sensors deployed within the ABACUS measuring campaigns. The overall number of hourly gaps across the growing season was overall very low for the branch bags system, and higher for the eddy covariance and the understorey chambers and the R2 of the daily models ranged between 0.7 and 0.8 (Table S2).

Table S2. Percentage of hourly gaps that had to be imputed using hourly or daily models of evaporative fluxes as a function of VPD and PAR. The R^2 of daily models is also shown.

	% of hourly gaps	**Daily model R^2**
Abisko		
T_{birch}	6%	Not needed
ET_{eco}	37%	0.70
Kevo		
T_{birch}	6%	0.79

ET_{eco}	25%	0.80
ET_{lichen}	44%	0.69
ET_{shrub}	42%	0.69

S5. Technical description of the automated chamber system for measuring tundra evapotranspiration

In Kevo, at *ca.* 150 m from the eddy flux tower, we deployed 12 PVC collars (19.9 cm internal diameter and 4.5 cm height) in early June 2008 to measure four microsite types of tundra communities, with three replicates for each type (cf. Table 1 in Poyatos et al. 2014). Three microsite types were dominated by tundra shrubs and differed in their spatial location, both in terms of microtopography and position along the mire to forest ecotone (Poyatos et al., 2014).

We used a closed dynamic gas exchange system for measuring H_2O flux rates (mmol H_2O m^{-2} s^{-1}). The system comprised an infra-red gas analyser (Li-Cor 8100, Li-Cor Inc., Lincoln, Nebraska, USA), a custom-built multiplexed gas handler unit (Electronics Workshop, Biology Department, University of York, UK) and 12 clear, Perspex chambers based on a commercial soil respiration model (LiCor 8100-101; 20 cm diameter). Chambers closed and opened sequentially, allowing hourly measurement cycles of 12 vegetation patches at a maximum radial distance of 20 m from the multiplexer. The chamber bases had rims with a rubber gasket, which ensured a tight fit with PVC collars. These collars were deployed on the 12 selected patches and gently sealed to the ground, without cutting or inserting into the substrate, using non-setting plumber's putty (Plumber's Mait, Bostik Ltd., Leicester, UK). We took this precaution to avoid damaging the prostrate stems and the roots of dwarf-shrub tundra species, which could potentially affect measured fluxes. The system operated from the 11th of June (DOY 163) until the 14th of September (DOY 258) of 2008.

Evapotranspiration from the chamber $ET_{chamber}$(mmol H_2O m^{-2} s^{-1}) was calculated as:

$$ET_{chamber} = \frac{P_{chamber}\,V_{chamber}}{RT_{chamber,0}}\frac{d}{dt}[H_2O]_{chamber} \qquad \text{(Eq.S2)}$$

where $P_{chamber}$ is air pressure inside the chamber (Pa), $V_{chamber}$ (m^3) is the system volume (chamber, irga/multiplexer and tubing), $T_{chamber,0}$ (°C) is air temperature at chamber closure, R (J K^{-1} $mmol^{-1}$) is the ideal gas constant, $A_{chamber}$ is chamber surface area (m^2) and d[H_2O]/dt (mmol $mol^{-2}s^{-1}$) is the rate of change in water vapour in the chamber headspace. We calculated this rate from water vapour concentrations measured every 2 seconds, over the 150 s period when the chamber remained closed. We estimated d[H_2O]/dt from the first order term of a quadratic fit between [H_2O] and time since chamber closure. Nonlinear fits describe better the concentration dynamics in the closed chamber, and do not systematically underestimate the fluxes. However, in the presence of noisy concentration data under low flux conditions, we opted for the more stable linear fit; we selected the linear regression whenever the slope for the linear fit and the linear term of the quadratic fit had opposite signs (cf. Supporting Information S2).Because of microclimatic alterations, water vapour sorption in the tubing system and imperfect chamber sealing the automated chamber system used here has been reported to underestimates the evaporative fluxes (Cohen et al., 2015).Therefore, we applied a correction factor of *ca.* 2.3, obtained in this latter study, which used a similar device under comparable environmental conditions (Cohen et al., 2015).

S6. Seasonal variation in the daily patterns of evaporative fluxes

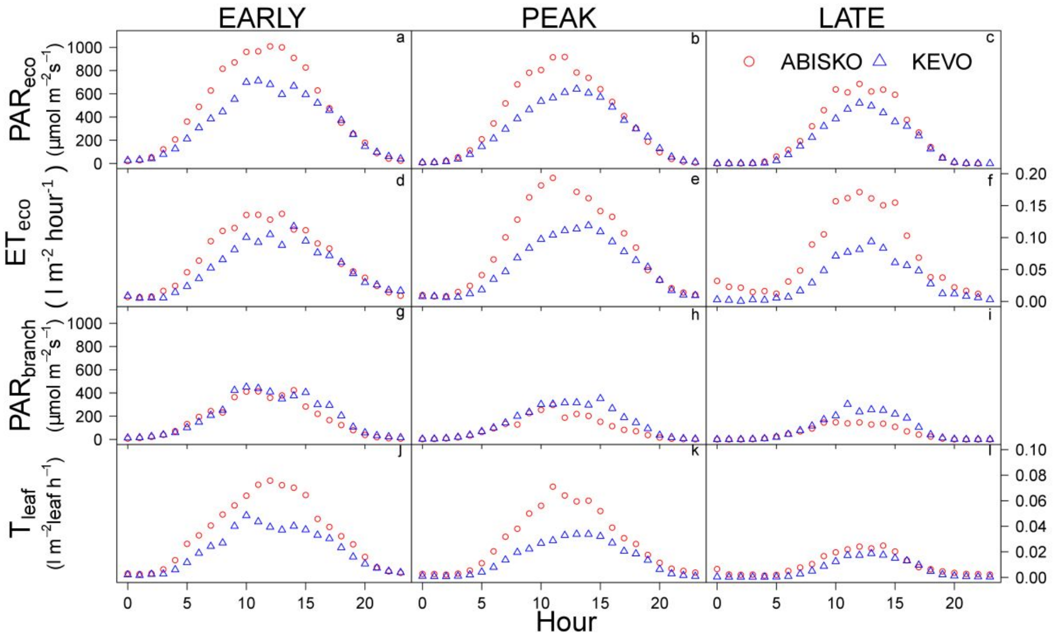

Figure S2. Seasonal variation in the mean daily patterns of ecosystem evapotranspiration (*ET_{eco}*) and birch transpiration per unit leaf area (*T_{leaf}*) compared to mean daily variation in PAR at the corresponding measurement scale. The growing season was split into three distinct periods according to leaf phenology (Early: 153-185, 171-185; Peak: 186-225, 186-230; Late: 226-241, 231-257, DOY in Abisko and Kevo, respectively).

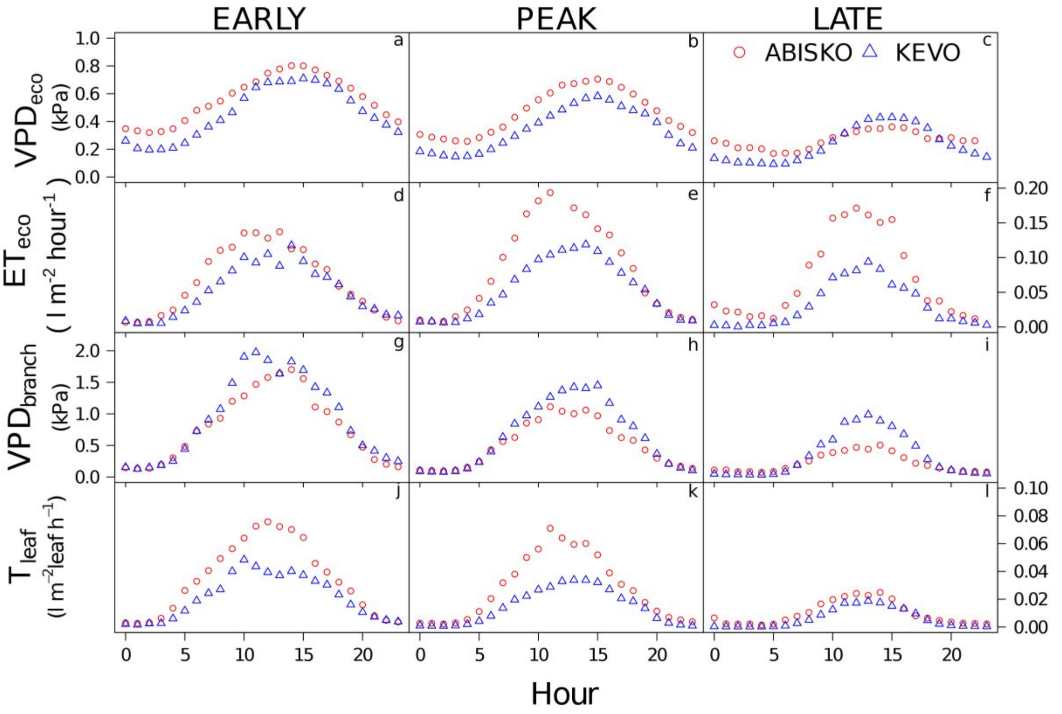

Figure S3. Seasonal variation in the mean daily patterns of ecosystem evapotranspiration (ET_{eco}) and birch transpiration per unit leaf area (T_{leaf}) compared to mean daily variation in VPD at the corresponding measurement scale. The growing season was split into three distinct periods according to leaf phenology (Early: 153-185, 171-185; Peak: 186-225, 186-230; Late: 226-241, 231-257, DOY in Abisko and Kevo, respectively).

S7. Footprint modeling

The contribution of different land cover types to the eddy covariance source area was estimated using an analytical footprint model (Hsieh, Katul, & Chi, 2000) assuming lateral dispersion (Detto, Montaldo, Albertson, Mancini, & Katul, 2006; Schmid, 1994). To save computation time a look-up-table approach was used (Crawford, Grimmond, Ward, Morrison, & Kotthaus, 2017), where the observed meteorological conditons at each 30-min timestep were matched to the pre-calculated land cover composition. Intervals of 15°, 0.2 m s^{-1} and 0.5 m s^{-1} were used for wind direction, friction velocity, and standard deviation of lateral wind, respectively; and three stability classes accounted for stable, unstable and neutral conditions. Typically, more than 80% of the source area was located within 500 m of the tower, with the peak contribution at a distance of about 23 m (36 m) in unstable (stable) conditions. As the land cover around the tower is a mixture of lichen, shrubs and birch, the variation in footprint composition with atmospheric conditions is small. (e.g. there is a slightly larger contribution from lichen for northeasterly winds and from trees for southwesterly winds, and the contribution of graminoid lawns and vascular plants near water is greater under stable conditions than unstable conditions).

The average footprint composition for the study period (DOY 160-260) is shown in Table S2 (percentage contributions have been scaled to give a total of 100%). Trees form the largest contribution (40%), followed by understorey (29%), followed closely by lichen (25%), with other land cover types contributing only a few percent at most.

Table S3: Average footprint composition for the study period in Kevo.

Land cover type	Average contribution to footprint [%]
Lichen	25.1
Vascular plants near water	3.4
Graminoid lawns	2.3
Understorey	29.1
Sphagnum	< 0.1
Trees	39.6
Road, boardwalk, powerlines	0.1
Open water	0.5

S8. Evapotranspiration upscaling using fixed and dynamic footprint

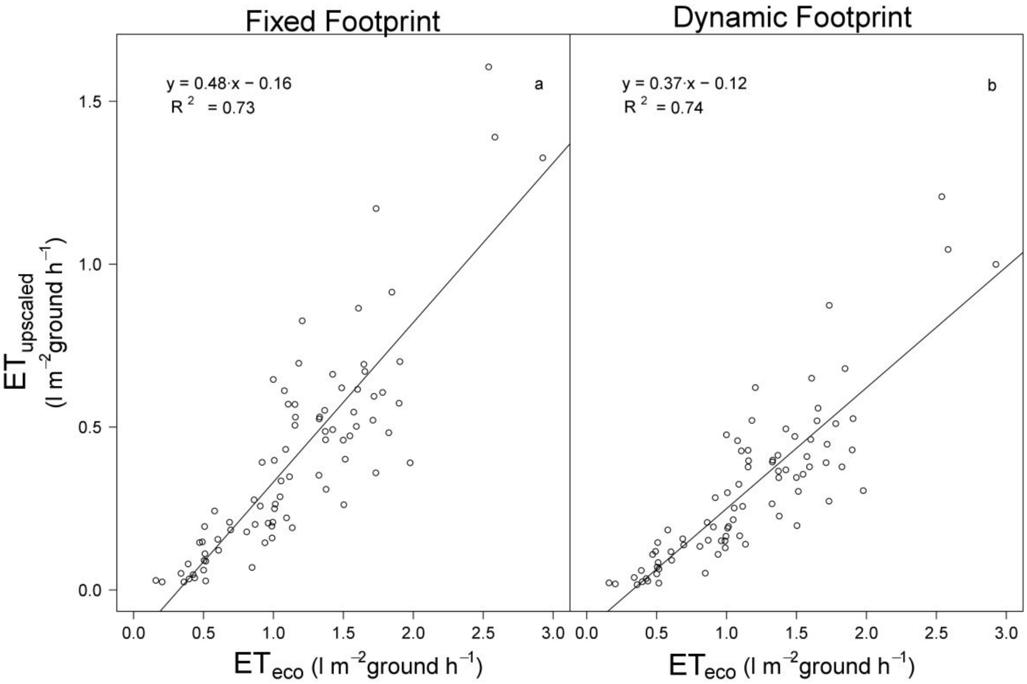

Figure S4. Linear regressions between ET_{eco} and $ET_{upscaled}$ using a fixed (a) or (b) dynamic footprint approach.

S9. Variation of daily T_{birch} / ET_{eco} in response to VPD_{eco}, PAR_{eco} and SMD.

Table S4. Linear models of T_{birch} / ET_{eco} in response to VPD, PAR and SMD after applying AIC-based model selection (cf. Methods). The reference level in this model is Abisko and significance codes are: $^{*}p<0.05$, $^{**}p<0.01$, $^{***}p<0.001$.

VPD model

	Estimate	SE	t-value	*p*
(Intercept)	42.896	1.781	24.079	$< 2 \cdot 10^{-16}$ ***
log(VPD)	12.554	1.689	7.432	$6.19 \cdot 10^{-12}$ ***
siteKevo	-18.863	2.890	-6.527	$8.56 \cdot 10^{-10}$ ***
log(VPD) : siteKevo	-4.661	2.390	-1.950	0.053

PAR model

	Estimate	SE	t-value	*p*
(Intercept)	-39.354	13.191	-2.984	0.0033 **
log(PAR)	11.981	2.223	5.391	$2.5 \cdot 10^{-7}$ ***
siteKevo	12.023	16.555	0.726	0.469
Log(PAR) : siteKevo	-4.340	2.887	-1.508	0.133

SMD model

	Estimate	SE	t-value	*p*
(Intercept)	33.435	1.256	26.62	$< 2 \cdot 10^{-16}$ ***
siteKevo	-18.454	1.679	-10.99	$< 2 \cdot 10^{-16}$ ***

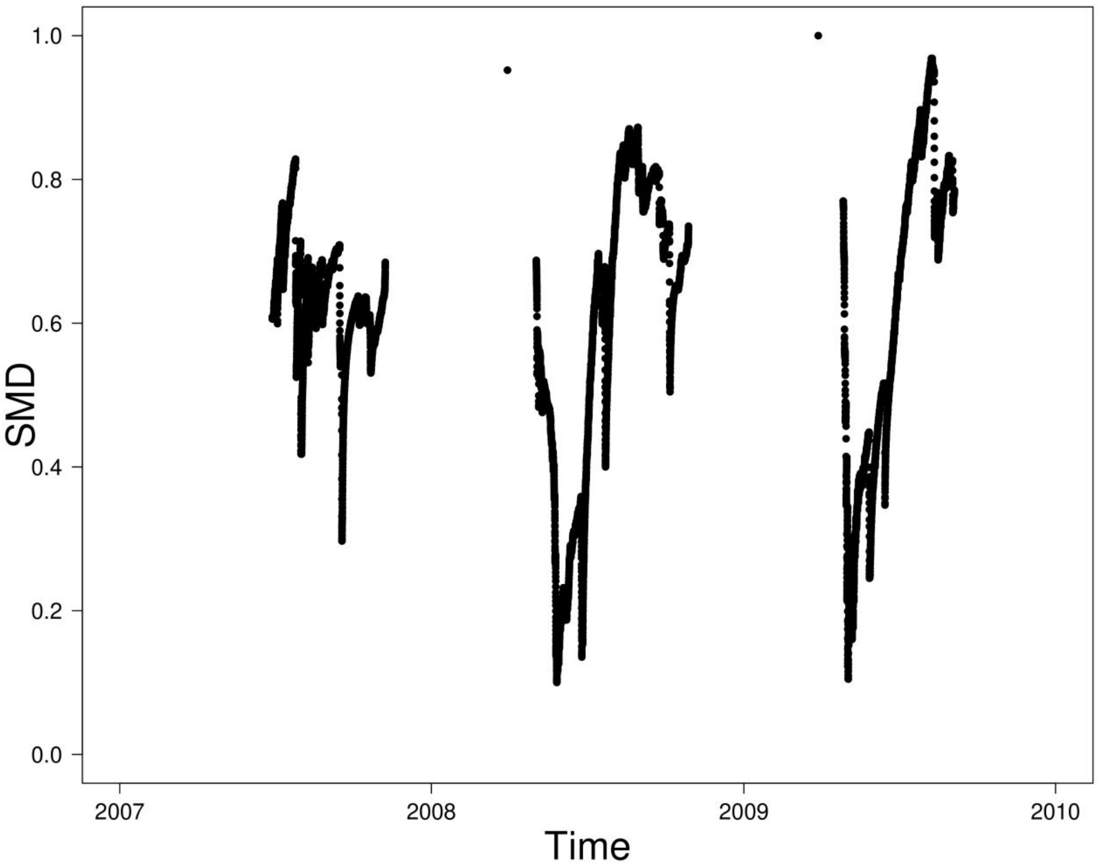

175 **S10. Soil moisture deficit dynamics in Abisko in 2007 - 2009**

176 **Figure. S5**. Soil moisture deficit (SMD) in Abisko in 2007 – 2009 showing the continuous increase after snowmelt in 2008 and 2009. 177

178

References

Cohen, L. R., Raz-Yaseef, N., Curtis, J. B., Young, J. M., Rahn, T. A., Wilson, C. J., … Newman, B. D. (2015). Measuring diurnal cycles of evapotranspiration in the Arctic with an automated chamber system. *Ecohydrology*, *8*(4), 652–659. https://doi.org/10.1002/eco.1532

Crawford, B., Grimmond, C. S. B., Ward, H. C., Morrison, W., & Kotthaus, S. (2017). Spatial and temporal patterns of surface–atmosphere energy exchange in a dense urban environment using scintillometry. *Quarterly Journal of the Royal Meteorological Society*, *143*(703), 817–833. https://doi.org/10.1002/qj.2967

Detto, M., Montaldo, N., Albertson, J. D., Mancini, M., & Katul, G. (2006). Soil moisture and vegetation controls on evapotranspiration in a heterogeneous Mediterranean ecosystem on Sardinia, Italy. *Water Resources Research*, *42*(8). https://doi.org/10.1029/2005WR004693

Hsieh, C.-I., Katul, G., & Chi, T. (2000). An approximate analytical model for footprint estimation of scalar fluxes in thermally stratified atmospheric flows. *Advances in Water Resources*, *23*(7), 765–772. https://doi.org/10.1016/S0309-1708(99)00042-1

Kutzbach, L., Schneider, J., Sachs, T., Giebels, M., Nykanen, H., Shurpali, N. J., … Wilmking, M. (2007). CO_2 flux determination by closed-chamber methods can be seriously biased by inappropriate application of linear regression. *Biogeosciences*, *4*(6), 1005–1025.

Poyatos, R., Gornall, J., Mencuccini, M., Huntley, B., & Baxter, R. (2012). Seasonal controls on net branch CO2 assimilation in sub-Arctic Mountain Birch (Betula pubescens ssp. Czerepanovii (Orlova) Hamet-Ahti). *Agricultural and Forest Meteorology*, *158–159*, 90–100. https://doi.org/10.1016/j.agrformet.2012.02.009

Poyatos, R., Heinemeyer, A., Ineson, P., Evans, J. G., Ward, H. C., Huntley, B., & Baxter, R. (2014). Environmental and Vegetation Drivers of Seasonal CO2 Fluxes in a Sub-arctic Forest–Mire Ecotone. *Ecosystems*, *17*(3), 377–393. https://doi.org/10.1007/s10021-013-9728-2

Schmid, H. P. (1994). Source areas for scalars and scalar fluxes. *Boundary-Layer Meteorology*, *67*(3), 293–318. https://doi.org/10.1007/BF00713146

Wagner, S. W., Reicosky, D. C., & Alessi, R. S. (1997). Regression models for calculating gas fluxes measured with a closed chamber. *Agronomy Journal*, *89*(2), 279–284.